

2005

Morphologic and stratigraphic evolution of the Antarctic Peninsula, Pacific margin

Jason Henry Holloman

Louisiana State University and Agricultural and Mechanical College

Follow this and additional works at: https://digitalcommons.lsu.edu/gradschool_theses



Part of the [Earth Sciences Commons](#)

Recommended Citation

Holloman, Jason Henry, "Morphologic and stratigraphic evolution of the Antarctic Peninsula, Pacific margin" (2005). *LSU Master's Theses*. 2753.

https://digitalcommons.lsu.edu/gradschool_theses/2753

This Thesis is brought to you for free and open access by the Graduate School at LSU Digital Commons. It has been accepted for inclusion in LSU Master's Theses by an authorized graduate school editor of LSU Digital Commons. For more information, please contact gradetd@lsu.edu.

MORPHOLOGIC AND STRATIGRAPHIC EVOLUTION OF THE ANTARCTIC
PENINSULA, PACIFIC MARGIN

A Thesis

Submitted to the Graduate Faculty of the
Louisiana State University and
Agricultural and Mechanical College
in partial fulfillment of the
requirements for the degree of
Master of Science

In

The Department of Geology and Geophysics

by
Jason Henry Holloman
B.S., Stephen F. Austin State University, 2002
December 2005

DEDICATION

I dedicate this work to my parents Henry B. Holloman Jr. and Susan Heard Holloman, who have stood by me through thick and thin (Keep Hope Alive). I also dedicate this work to the great state of Texas. From Orange to El Paso and from Brownsville to the Red River, I will always remember where I have come from.

ACKNOWLEDGEMENTS

I would first like to thank my advisor, Dr. Philip J. Bart, and my committee members, Dr. Juan Lorenzo and Dr. Mike Blum. Their help and guidance have made this study possible. I would also like to thank the Department of Geology and Geophysics, its Faculty and its Staff. I would like to thank my fellow graduate students for being like an extended family to me. I especially thank my family, who kept me going and pushed me to be the best. Special thanks also go out to Ms. Sharrisse Evans; thanks for all the support.

This project would not have been realized without the financial support of the National Science Foundation (NSF); the grant awarded to Dr. Bart enabled us to participate in data gathering cruises on Antarctic waters. I am grateful for the technical and logistical support provided by Raytheon Polar Services Company; Captain Joe Borkowski and the crews of the Research Vessel/Ice Breaker Nathaniel B. Palmer, Polar Duke; and Edison-Chouest Offshore.

TABLE OF CONTENTS

DEDICATION	ii
ACKNOWLEDGEMENTS	iii
LIST OF TABLES	v
LIST OF FIGURES	vi
ABSTRACT	vii
CHAPTER 1. INTRODUCTION	1
CHAPTER 2. METHODS	5
2.1 Seismic Reflection Data Set	6
2.2 Bathymetric Map.....	6
2.3 Seismic Tie to ODP Sites 1097 and 1103.....	7
CHAPTER 3. RESULTS	9
3.1 Bathymetry	9
3.2 Seismic Packages	11
3.3 Well Data	16
3.4 Mapping	18
CHAPTER 4. DISCUSSION	33
4.1 Evidence of Trough Mouth Fans	33
4.2 Evidence of a Relic Morphology – Transition from Progradation to Aggradation	34
4.3 Timing Constrained from ODP Shelf Sites	36
4.4 Possible Model for the Continental Shelf	36
CHAPTER 5. CONCLUSIONS	38
REFERENCES	39
APPENDIX A. TIME – DEPTH CONVERSIONS FOR ODP SITES.....	42
APPENDIX B. UNIT DISTRIBUTION MAPS FOR PACKAGES -1 AND -2	48
VITA	59

LIST OF TABLES

1. Position of seismic unconformities with respect to ODP site 109718
2. Position of seismic unconformities with respect to ODP site 110319

LIST OF FIGURES

1. Rebesco et al. (1998) Model	4
2. Bathymetric map of the Antarctic Peninsula continental shelf and rise	8
3. Seismic strike lines PD 88-B and NBP02-5	10
4a. Seismic strike lines NBP02-05 and PD 88-B	12
4b. Seismic strike lines NBP02 -03, and -06.....	13
5. Seismic dip lines 88 -1,-2,and -3	14
6. Seismic dip lines 88 -5, -7,and -10	15
7. Seismic correlation to ODP Site 1097	17
8. Seismic correlation to ODP Site 1103.....	20
9. Time-structure map of the top of Package 2	22
10. Time-structure contour map of the base of Package 2... ..	23
11. Time-structure contour map of unconformity 2.3.....	24
12. Time-structure contour map of unconformity 2.4.....	25
13. Time-structure contour map of unconformity 2.5.....	26
14. Distribution map of Package -2 units	27
14a. Distribution map of Unit 2.4	28
15. Distribution map of Package -1 units	29
15a.Distribution map of Unit 1.2	30
16. Time-thickness map of Package 1	31
17. Time-thickness map of unit 1.1	32
18. Paleo-reconstruction map	35
19. Model of deposition and morphology	37

ABSTRACT

Rebesco et al. (1998) proposed a general depositional model that relates sediment drift evolution on the Antarctic Peninsula Pacific-margin continental rise to glacial processes on the continental shelf. In their model, terrigenous sediment was directly delivered to the rise and contributed to the construction of large sediment drifts when grounded ice extended to the shelf edge. In this scenario, large volumes of fluidized sediment bypassed the margin at the mouth of ice streams (i.e., fast flowing ice), whereas prograding slopes were constructed on those portions of the shelf margin between major ice streams. This model relies heavily on the modern geomorphology of the margin.

In contrast, an evaluation of the subsurface stratigraphy suggested that there may have been significant lateral shifts of ice-stream locations and associated trough-mouth-fan depositional systems through time (Bart and Anderson, 1995). New seismic data was acquired along the strike of the Antarctic Peninsula shelf during the 2002 season aboard the NBP R/VIB. Detailed mapping and regional correlations confirm that slope progradation between the modern troughs was indeed associated with large ice streams. Moreover, the new mapping results presented here illustrate that the last several glacial cycles did not produce significant slope progradation anywhere along the margin. This signifies a major change in the stratal-stacking pattern on the outer continental shelf. Correlation with age control at ODP Leg 178 shelf sites 1097 and 1103 indicates that the shift from progradation to aggradation occurred at ~5 Ma (Pliocene).

CHAPTER 1. INTRODUCTION

It is important that both modern and past operations of the Antarctic cryosphere are understood to the fullest extent to best prepare for the future changes of Earth's climate and eustasy. Today, the ice volume of the Antarctic Peninsula is small ($230,000 \text{ km}^3$, i.e., less than a few cm in terms of sea-level equivalent; Denton et al., 1991) but during the last glacial maximum, the Antarctic Peninsula Ice Sheet (APIS) advanced across the broad continental shelves on the Atlantic and Pacific margins (Pope and Anderson, 1992; Sloan et al. 1995). With respect to the intermediate-sized West Antarctic Ice Sheet, and the large East Antarctic Ice Sheet, the APIS probably has added and lost the largest percentage of ice volume during recent glacial cycles. Moreover, as the northern most extension of the Antarctic cryosphere, the APIS probably has been extremely sensitive to climatic changes through the Neogene. Thus, despite its relatively small size, the APIS may play an important and dynamic role in terms of sea-level oscillations likely to affect humanity as well as bottom-water production, atmospheric circulation, etc.

Bathymetric studies by Canals et al. (2000) and Dowdeswell et al. (2004) of the well surveyed Pacific margin of the Antarctic Peninsula show the influence of the region's dynamic glacial history. The inner shelf is deeply eroded to crystalline basement and the outer shelf is characterized by large banks and broad, foredeepened glacial troughs oriented perpendicular to the margin. These valleys are the locations of former ice streams when grounded ice (ice in contact with the sea floor) advanced from land to the shelf edge. Ice streams are defined as fast flowing zones of an ice sheet bordered by slowly moving ice. Because of the rapid velocities (typically $>400 \text{ m year}^{-1}$) and large dimensions of ice streams ($>20 \text{ km}$ wide and $>150 \text{ km}$ long), these features account for a

large percent of ice volume discharge from the continent. The vigor with which these streams flow is a key control on ice sheet stability (Stokes, 2002).

The bathymetry of the outer shelf is characterized by four main lobes, which are bounded by sea floor troughs (Rebesco et al. 1998). In the subsurface, the continental shelf is generally progradational, with progradation concentrated at these four main lobes (Larter and Cunningham 1993). Material eroded from the continent and shelf were transported in subglacial debris zones to depocenters on the upper slope. These accumulations were called Trough Mouth Fans (TMF) by Vorren and Laberg (1997). TMFs are slope fans at the mouth of transverse troughs/channels on glaciated continental shelves.

Rebesco et al. (1998) proposed a model (Figure 1) that relates glacial processes on the shelf to drifts on the adjacent rise. Rebesco et al. (1998) inferred that the prograding wedges on the outer continental shelf represent boundaries between paleo-ice streams. Rebesco et al. (1998) also argued for limited lateral shifts of depositional systems on the shelf. In contrast, Bart and Anderson (1995) argued for significant lateral shifting of depositional systems during successive glacial cycles. The Rebesco et al. (1998) model is also in contrast with the Vorren et al. (1997) model, which suggested a depocenter at the mouth of the trough (i.e., ice stream). The Rebesco et al. (1998) model described a situation in which glacial melt water formed fine grained turbid surface plumes that settled on the upper slope (i.e. bypass of the shelf). Mass wasting on the slope became organized into a converging pattern of turbidity channels, which transported material basinward. On the lower rise, the fine grained suspension component of the turbidity currents were deposited in the sediment drifts, while the coarse traction components

continued to the lower rise-abyssal plain and formed deep sea fan deposits. Rebesco et al. (1998) also argued that in spite of the larger amount of sediment transported by basal meltwater to the mouth of the glacial troughs, the Antarctic Peninsula margin experienced minor progradation and a high degree of bypass and erosion at the trough mouths. They also did not recognize trough mouth fans or the morphologic expression of fan growth at the mouth of troughs. However, they noted that the existence of trough mouth fans on the margin is still an open question.

The model primarily is based on the geomorphology of the modern sea floor and thus there are two basic issues that need to be evaluated before the model can be accepted.

1) Previous work on the continental shelf shows that locations of ice streams shifted from glacial to glacial period (Bart and Anderson, 1995) and thus the position of slope progradation was not stationary.

2) Upper-slope progradation was only significant during one stratigraphic interval (Package 2 from Bart and Anderson, or Sequence 2 from Larer and Barker, 1989).

An understanding of the past processes that shaped the continental shelf, slope and rise of the Antarctic Peninsula Pacific margin is important to help decipher how fluctuations of the ice sheets on the Peninsula relate to ice volume changes elsewhere in Antarctica as well as to climate or eustatic phenomena evident in low latitude and deep sea records.

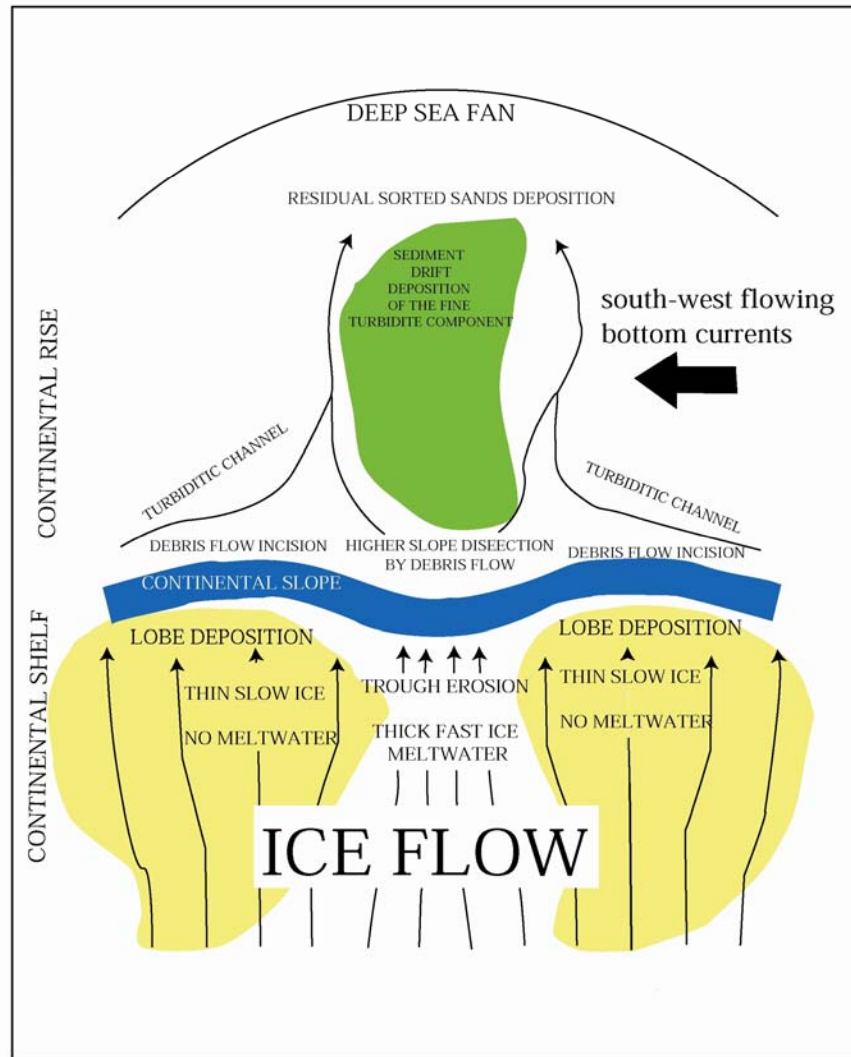


Figure 1: Rebesco et al. (1998) proposed a model that relates glacial processes on the shelf to drifts on the adjacent rise. The Rebesco et al. (1998) model infers that the prograding wedges on the outer continental shelf represent boundaries between paleo-ice streams. Figure modified from Rebesco et al. (1998).

The objectives of this study are:

1. To evaluate the Rebesco et al. (1998) model on the basis of subsurface stratigraphy using a newly acquired data set.
2. Constrain the timing of continental shelf evolution the continental shelf through correlation with age control at ODP Leg 178 shelf sites.

CHAPTER 2. METHODS

Four experiments were performed to evaluate the Rebesco et al. (1998) model. First, the subsurface stratigraphy, stratal relationships and geometries were imaged using 2D single channel seismic (SCS) data. Second, a bathymetric map was created using the first arrivals from the seismic data and ship board multibeam systems. Third, the seismic packages were mapped for thickness and structure to constrain distribution and morphology of the key seismic reflectors. Fourth, data from ODP Leg 178 drill sites on the shelf were analyzed to establish seismic correlations with the lithostratigraphy and biostratigraphy to constrain processes and timing of grounding events on the continental shelf. To test the validity of the Rebesco et al. (1998) model for the evolution of the continental shelf, the data were examined for the following:

1. Cross-cutting stratal relationships indicating ice-sheet advance over previously deposited sediments and the location of paleo-ice streams.

Key seismic reflectors were interpreted on strike oriented seismic profiles.

2. Correlation of upper-slope progradation on the outer shelf to cross-cutting stratal relationships on the mid- to inner shelf regions.

Key seismic reflectors that indicated cross cutting relationships on the middle shelf were correlated to the upper slope to establish the relationship between cross-cutting and upper slope progradation or aggradation.

3. Distribution of unconformities and packages. Comparison with modern bathymetry to the seismic packages.

The distribution of seismic packages and key reflectors were measured from the seismic data at an interval of ~2.5 km. These points were then hand contoured and compared to the modern bathymetry.

2.1 Seismic Reflection Data Set

The three grids used in this study were acquired with either one or two 100 cubic inch water guns (PD88) or a 100 cubic inch generator-injector airgun (PD90 and NBP02). The original Package-1 and -2 seismic interpretations (by Bart and Anderson from PD88 and PD90) were correlated to the new NBP02 seismic profiles. The NBP02 grid contains 5500 km of regional strike-oriented SCS transects on the outer continental shelf. An iterative process of tracing beds around loops defined by adjacent dip-oriented and strike-oriented seismic profiles was performed to confirm that laws of superposition were not violated. Base maps for seismic and ODP Leg 178 sites were generated in Mercator projection using Didger mapping software. Data points for Package-1 and -2 unconformity contour maps (time elevations with respect to sea level) were measured by hand from paper seismic profiles and transferred to seismic-transect base maps. The horizon-elevation data was hand-contoured at 50 millisecond contour intervals.

2.2 Bathymetric Map

A bathymetry map was constructed using first arrivals from the seismic data set and multi-beam measurements. These data points were measured in milliseconds and contoured by hand at a 20 msec contour interval. The time contours were then converted to meters using 1500 m/s as the velocity of sound in water with a contour interval of 50m. The data from this study were merged with data from portions of the continental slope and rise from the Rebesco et al. (1998) bathymetry map.

2.3 Seismic Tie to ODP Sites 1097 and 1103

The individual seismic reflectors interpreted as glacial unconformities within Packages -1 and -2 were projected to the core-based sedimentologic and diatom-based biozones at Leg 178 Sites. To convert seismic-reflection times of the Packages -1 and -2 unconformities to depth, I evaluated the existing velocity information provided in Leg 178 Initial and Science Report. I used a detailed two-way-travel time (TWTT) - depth conversion table created by Bart et al. (accepted) (Appendix A) for Site 1097 using the 42 measurements of P-wave-velocity from a Hamilton-Frame sensor pair, PWS3 for core recovered at Site 1097 (Shipboard Scientific Party, 1999). At Site 1103, I used TWTT-depth conversions for Package -1 glacial unconformities by utilizing the Tinivella et al. (2001) velocity and an analysis of the time depth conversion done by Bart et al. (accepted) for this site. At Site 1103, Tinivella et al. (2001) subdivided a dip-oriented cross section (passing through the Site-1103 location) into seven layers (their Figs. 6e and 7e). Using their derived 7-layer velocity model for this site, Bart et al. (accepted) converted the TWTT for the tops and bases of the seven layers defined by Tinivella et al. (2001) to depth by working from the sea floor downward. Knowing the TWTT of Packages-1 seismic reflectors (with respect to the TWTT, depth, and velocity layering defined by Tinivella et al. (2001)) allowed Bart et al. (accepted) to convert the Packages-1 seismic-reflection times to depth below seafloor at Site 1103. I did not use Sites 1102 and 1100 on the northeastern continental shelf because of limited penetration and recovery of Packages -1 and -2.

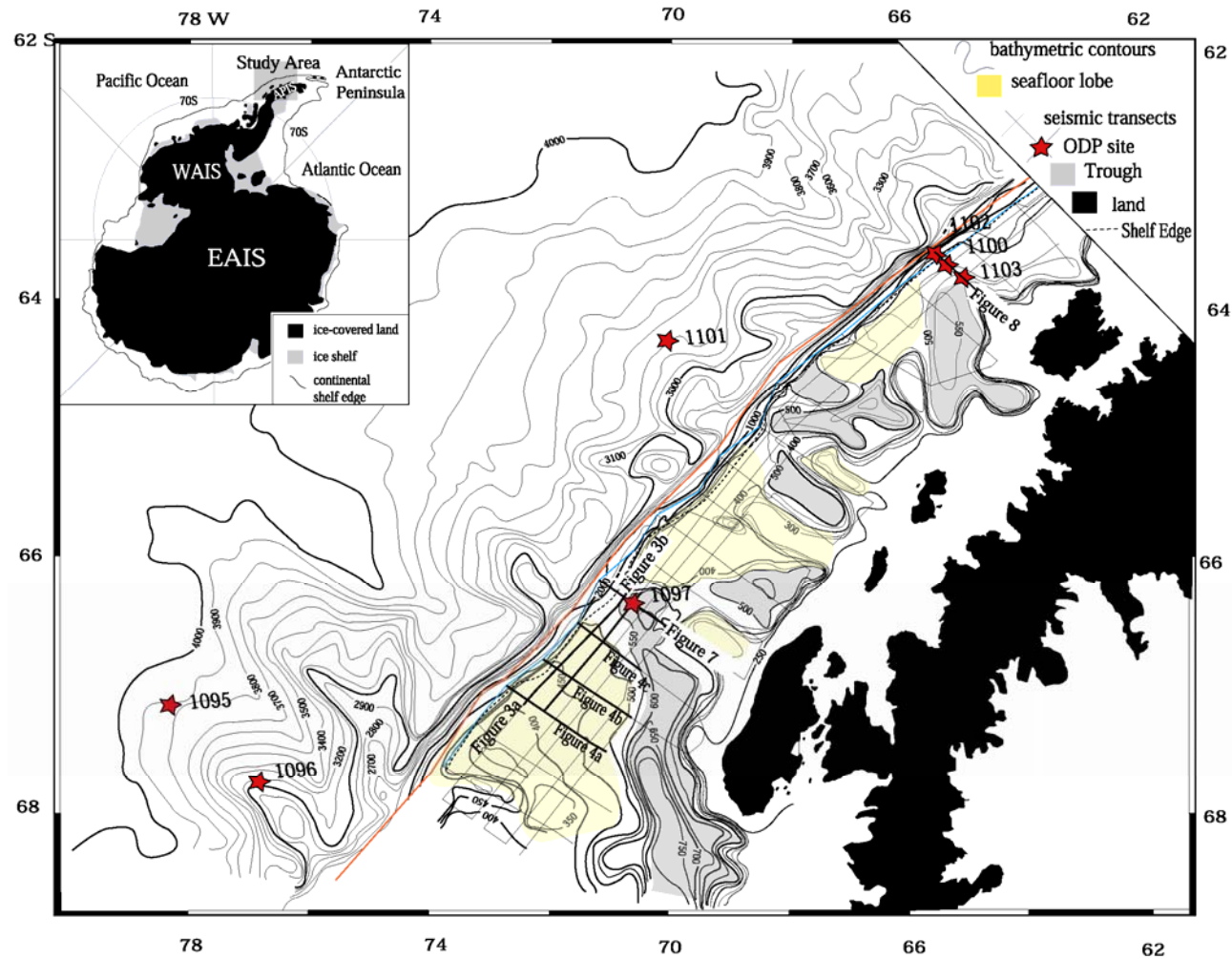


Figure 2: Bathymetry map was constructed using first arrivals from the seismic data set and multi-beam measurements. These data points were measured in milliseconds and contoured by hand at a 20 msec contour interval. The time contours were then converted to meters using 1500 m/s as the velocity of sound through water with a contour interval of 50 m. Contour interval of 100 m signified by bold contours. The shelf edge is designated by the dotted black line. The data from this study was merged with data from portions of the continental slope and rise from the Rebesco et al (1998) bathymetry map. A light blue solid line designates the basinward most point where the data I generated from the seismic grid ends. A red solid line indicates the landward most limit of contours from Rebesco et al. (1998). The zone between these two lines was used to merge the two data sets and connect contours.

CHAPTER 3. RESULTS

3.1 Bathymetry

The bathymetric map generated in this study (Figure 2) was compared to the bathymetric map constructed by Rebesco et al. (1998). The map (Figure 2) reveals a trough and bank morphology. The light blue solid line designates the basinward most point of the contour map generated from the seismic grids used in this study. The red solid line indicates the landward most limit of contours from Rebesco et al. (1998). The zone between these two lines represents the area over which the two data sets were merged. Contours from this study were connected with those from Rebesco et al. (1998).

The most prominent feature on the shelf is Marguerite Trough which deepens to over 600 meters. The shelf is also characterized by large lobes that protrude portions the shelf edge. The map created in this study shows the same general bathymetry reported by Rebesco et al. (1998) . However, the map in this study uses dense outer-shelf control and thus smaller contour intervals help better resolve trough and bank relationships on the shelf. For example, the presence of a sediment ridge in the southwestern region of the study area is better resolved on the new map than the Rebesco et al. (1998) map.

Dowdeswell et al. (2004) used multibeam data to image features on the outer continental shelf and rise. The morphology of the upper continental slope consists of a series of gullies, running in an almost unbroken sequence across the mouth of Marguerite Bay (Dowdeswell et al., 2004). Dowdeswell et al. (2004) also stated that there is lack of deep canyons cutting into the shelf and slope on that sector of the Antarctic Peninsula margin adjacent to Marguerite Bay.

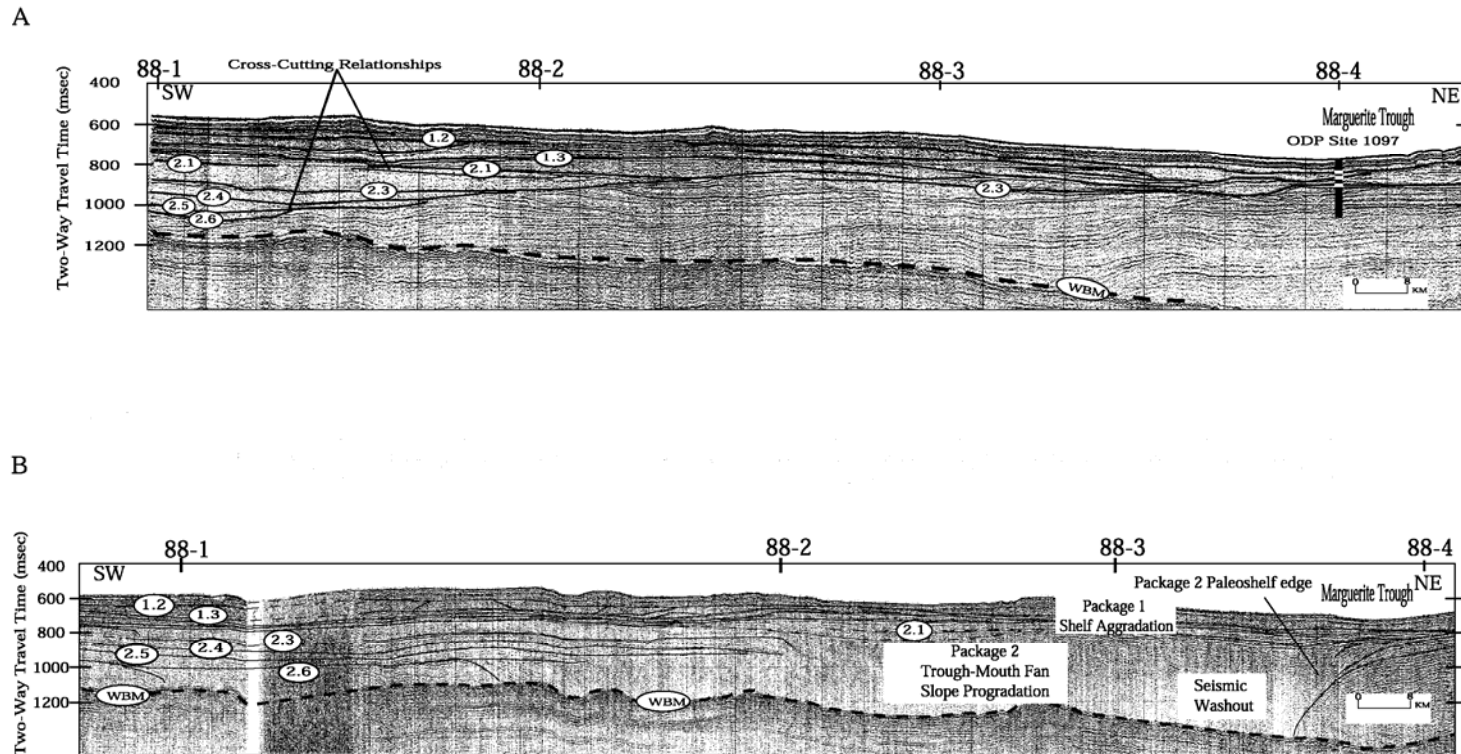


Figure 3: A) Seismic line 88 B is an inner shelf strike line that ties with 88-1, 2, 3 and 4. In line 88 B cross cutting reflectors are present in packages one and two. These cross cutting relationships have been interpreted as paleo-troughs, the former locations of ice streams. These paleo troughs indicate that ice streams and therefore troughs have shifted through time. These paleo-troughs are up dip from the package two upper slope progradation. B) Seismic line 02-5 is the outer most strike line in the data set. This portion of the line crosses the lobe to the west of Marguerite Trough. The lower units of package two contain laterally accreting foresets which correlate to progradation on dip lines (88-1, 88-2, and 88-3 (Figure 4). The foresets dip into a large zone of seismic washout. Units 2.3-2.6 all dip into this zone of seismic washout. Unconformity 2.1 marks the transition to an aggradational setting and this continues through package one.

3.2 Seismic Packages

Package 1 (S1 of Larter and Barker, 1989) is the upper most package in the sedimentary sequence. Package 1 is characterized by strong parallel reflectors throughout and consists of three aggradational units (Units 1.1, 1.2 and 1.3) bounded by glacial unconformities. The package shows minimal progradation at the shelf edge (Figure 5 a,b and c). There are also cross-cutting relationships present in Package 1.

Package 2 underlies Package 1 and consists of 10 units that are bounded by glacial unconformities (Unconformities 2.1 to 2.10). Package 2 is characterized by large amounts of outer shelf/upper slope progradation. The deeper units of Package 2 have a greater degree of outer shelf/upper slope progradation than the upper units of the package, which transition into an aggradational pattern (Figure 5 a,b,and c). Progradation in this package is characterized by prograding foresets and steeply dipping reflectors on dip lines at the shelf edge (Figure 5 a,b,and c). In strike line 5 (Figure 3b) across the outer continental shelf, the package is defined by laterally accreting foresets that can be correlated to the progradation foresets observed in dip lines (Figure 5 a,b, and c) on the outer continental shelf. The progradation is focused in areas that form morphologic bulges at the continental shelf/slope break. In the subsurface of the inner and mid continental shelf, cross cutting relationships in the form of truncated glacial unconformities are present (Figure 3a). Only portions of the unconformities remain due to erosion during subsequent ice sheet expansions, and erosion. The cross cutting relationships occur up dip of the outer shelf/upper slope progradation. Extent of seismic units and unconformities can be seen in Figure 4. This figure shows the lateral extent of truncation and crosscutting along strike.

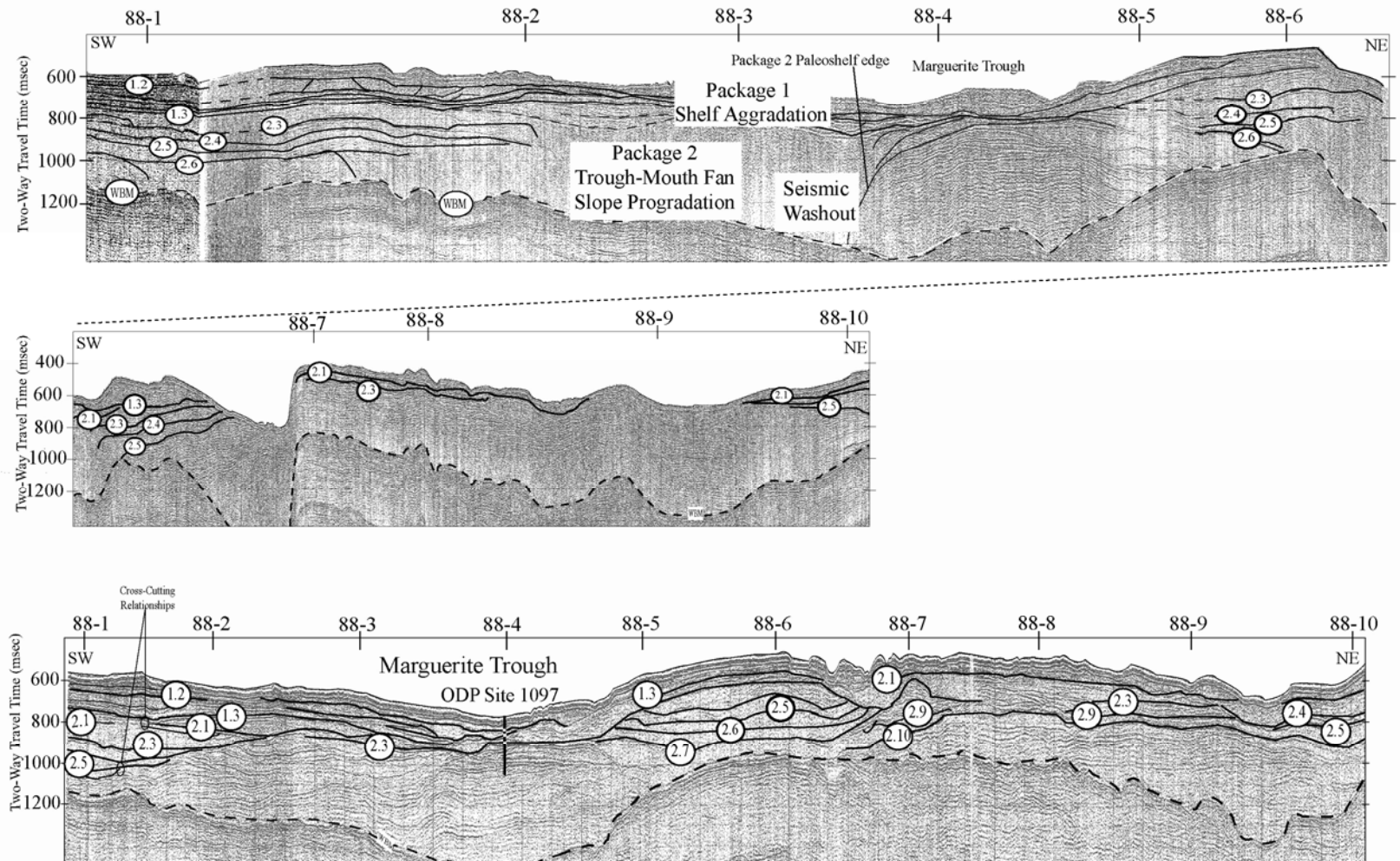


Figure 4a: Southwest-northeast (strike-oriented) regional seismic profiles NBP 05-02, PD 88B, on the outer and middle continental shelf (see figure 1 for location) Dotted line is water bottom multiple

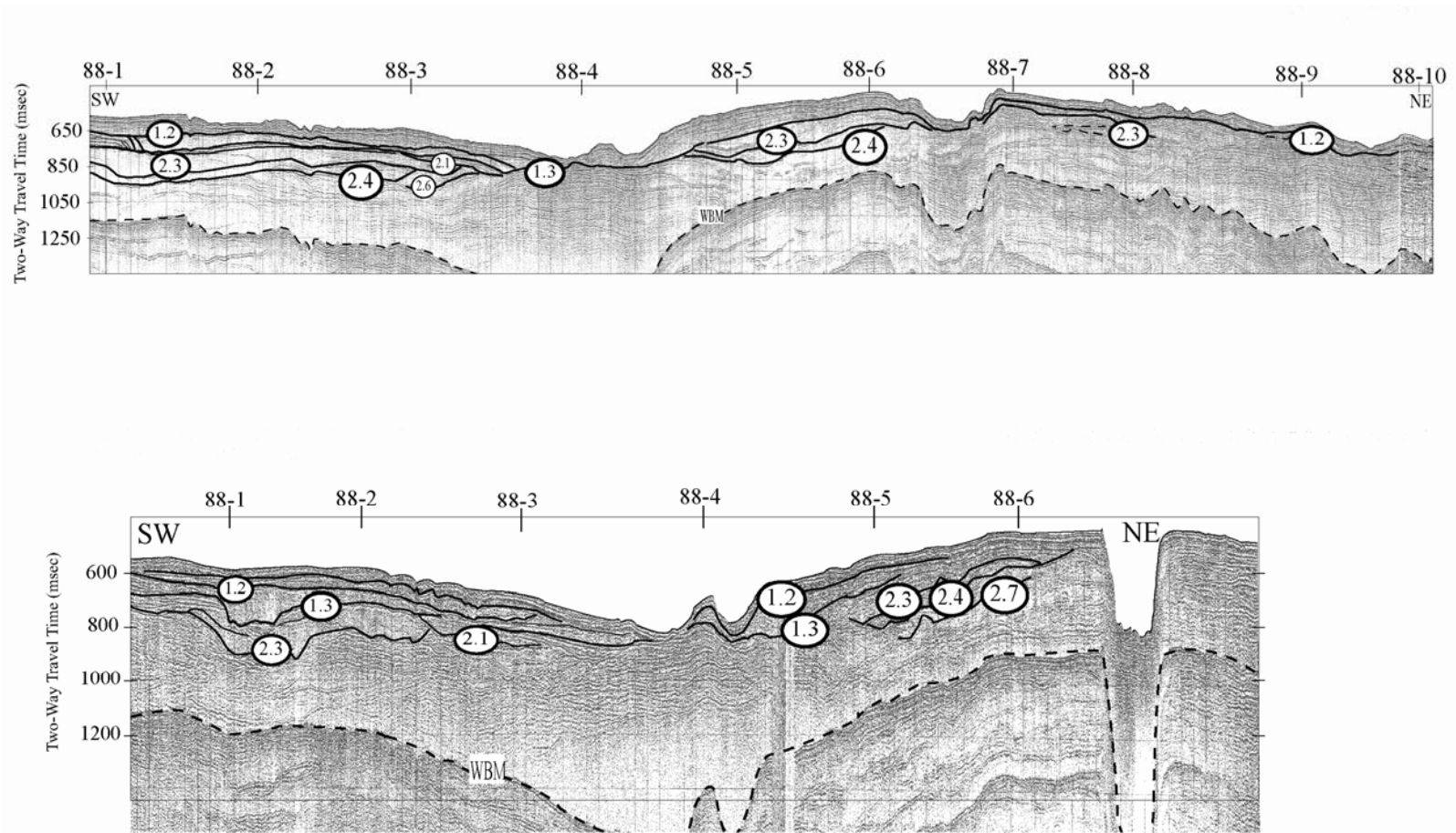


Figure 4b: Southwest-northeast (strike-oriented) regional seismic profiles NBP 02-03, and NBP 02-06 on the middle continental shelf (see figure 1 for location) Dotted line is the water bottom multiple.

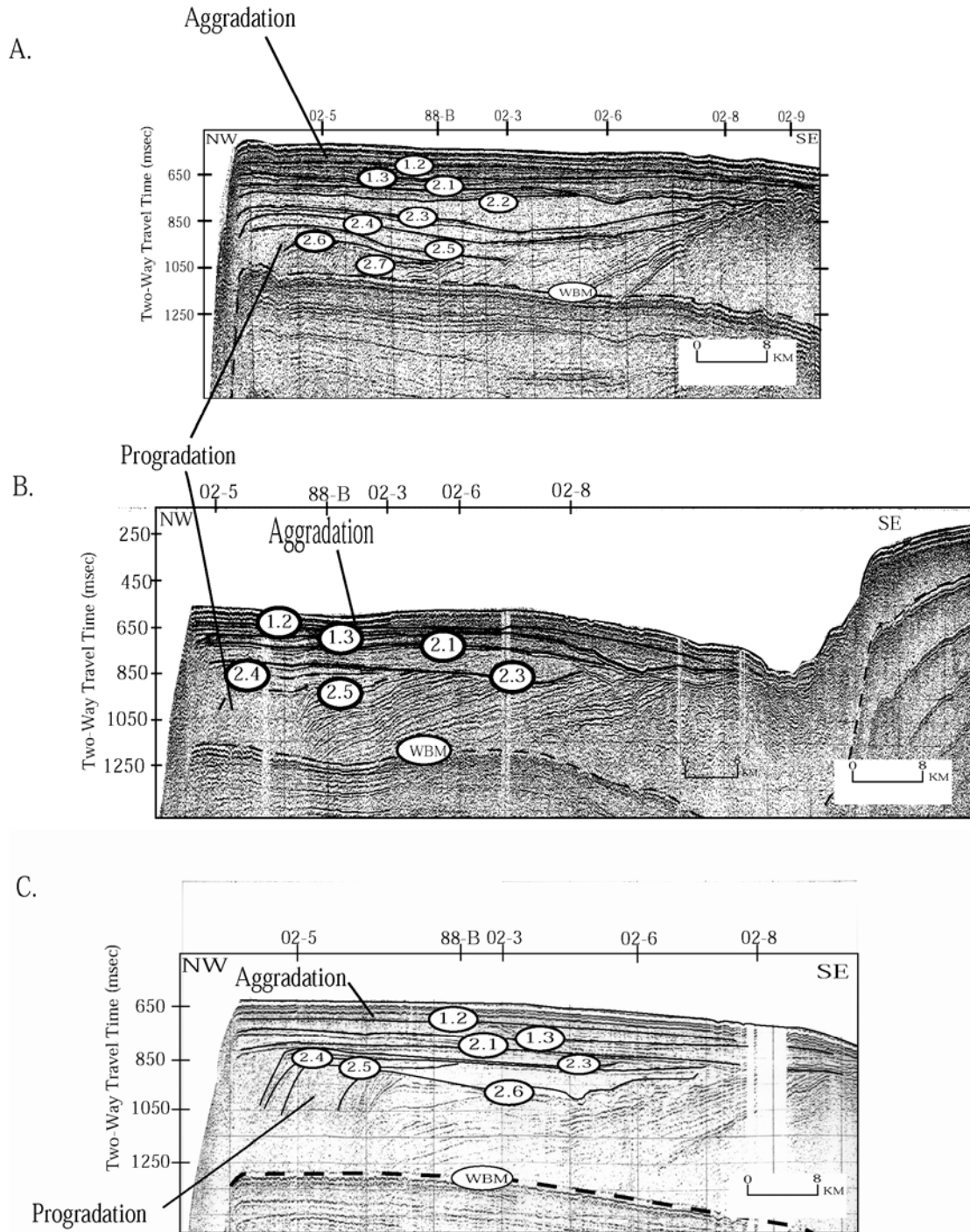


Figure 5: Seismic lines (a) 88-1, (b) 88-2, and (c) 88-3 are dip oriented lines that cross the most western lobe in this study. These lines indicate major upper slope progradation in the lower units of package - 2. Unconformities 2.3 and 2.1 begin an upward zone of parallel reflectors that continue into package one and have been interpreted as aggradational in nature. This upper slope progradation is also coincident with the position of lobe 4 morphology exhibited at the sea floor.

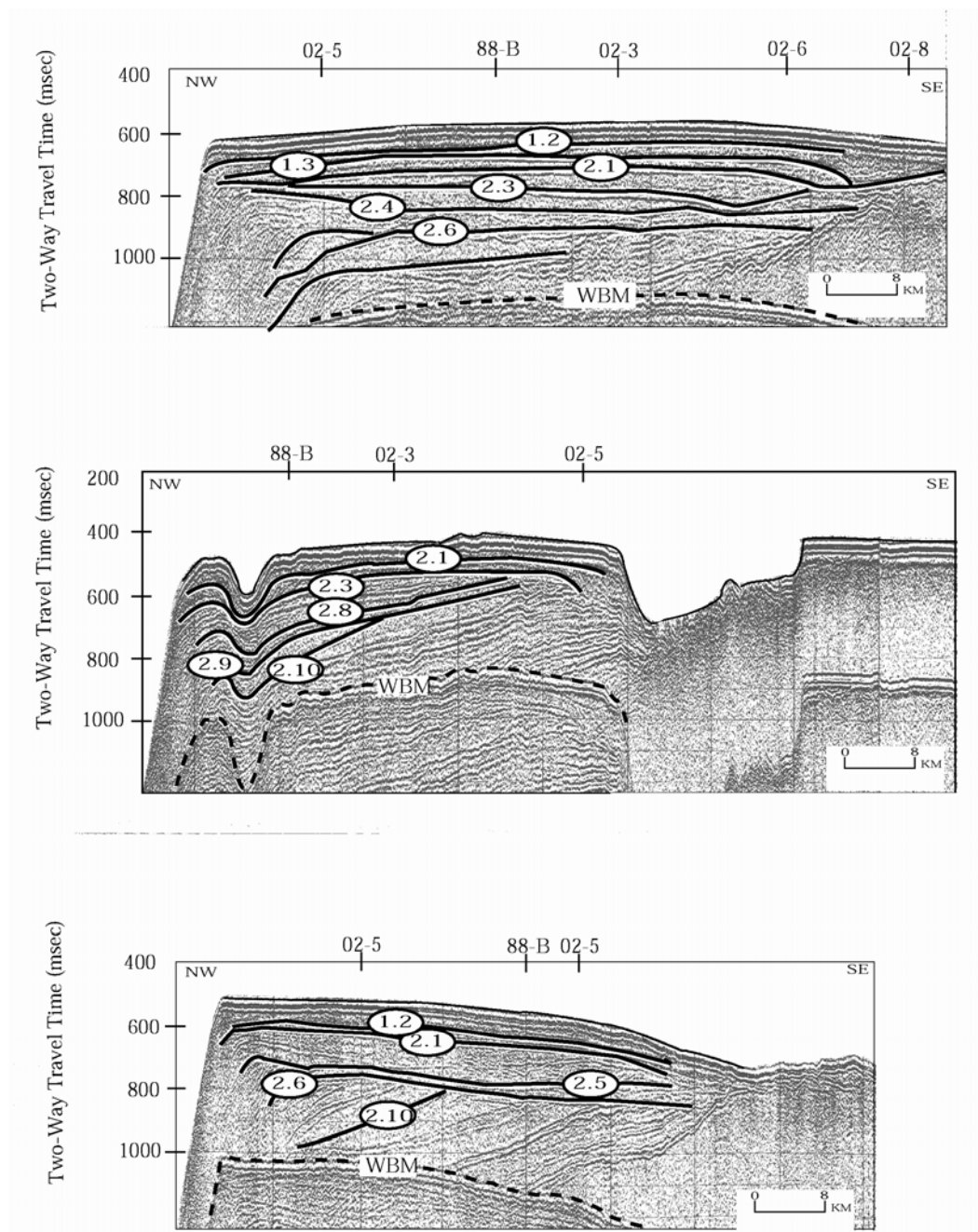


Figure 6: Northwest-southeast (dip-oriented) seismic profiles PD-88-5, PD-88-7, and PD-88-10 on the outer and middle continental shelf . Dotted line is the water bottom multiple.

3.3 Well Data

The ODP Site 1097A (Figure 7) on the continental shelf is between depositional lobes 3 and 4. Site 1097A was positioned at the tie point between strike line 88-B and dip line 88-4. This permits correlation to the biostratigraphic age control from this hole. The site penetrated to 436.60 m below the sea floor (mbsf) with a recovery of 13.58 percent. The oldest strata sampled was a Late Miocene diamict. The base of Package 1 is at 108 mbsf and the base Package 2 is at 178 mbsf in Site 1097. The final 28 meters of Package 1 lie within the *Thalassiosira inura* zones (subzone b). The *Thalassiosira inura* Zone (subzone b) is dated between 4.25 and 5.12 Ma (Winter and Iwai, 2001). The top of Package 2 (unit 2.1) also lies within the *Thalassiosira inura* zone (subzone b). The last 40 meters of Package 2 sampled at Site 1097 correlate to the *Thalassiosira inura* Zone (subzone a) which is dated between 5.12 Ma and 5.55 Ma (Winter and Iwai, 2001).

Massive matrix supported diamictite represents the most common sediment type identified at Site 1097 comprising some 65% of the total cumulative length of core recovered (Eyles et al., 2001). The term diamictite refers to poorly sorted and lithified admixtures of clasts (defined as larger than sand-sized) and matrix fines (Eyles et al., 2001). A majority of the core recovered at Package 1 and 2 intervals was interpreted by the Shipboard Party (1999) as diamict. Massive diamictite facies recovered within the uppermost 150 m of the hole are characterized by relatively low porosities interpreted by the Shipboard Party (1999) as the result of subglacial shear consolidation. ODP site 1103 (Figure 8 a,b) is located on the northeastern part of the continental shelf. ODP Site 1103 sample Packages 1 and 3. Package-2 is absent at this location. Like Site 1097, Site 1103 had poor recovery.

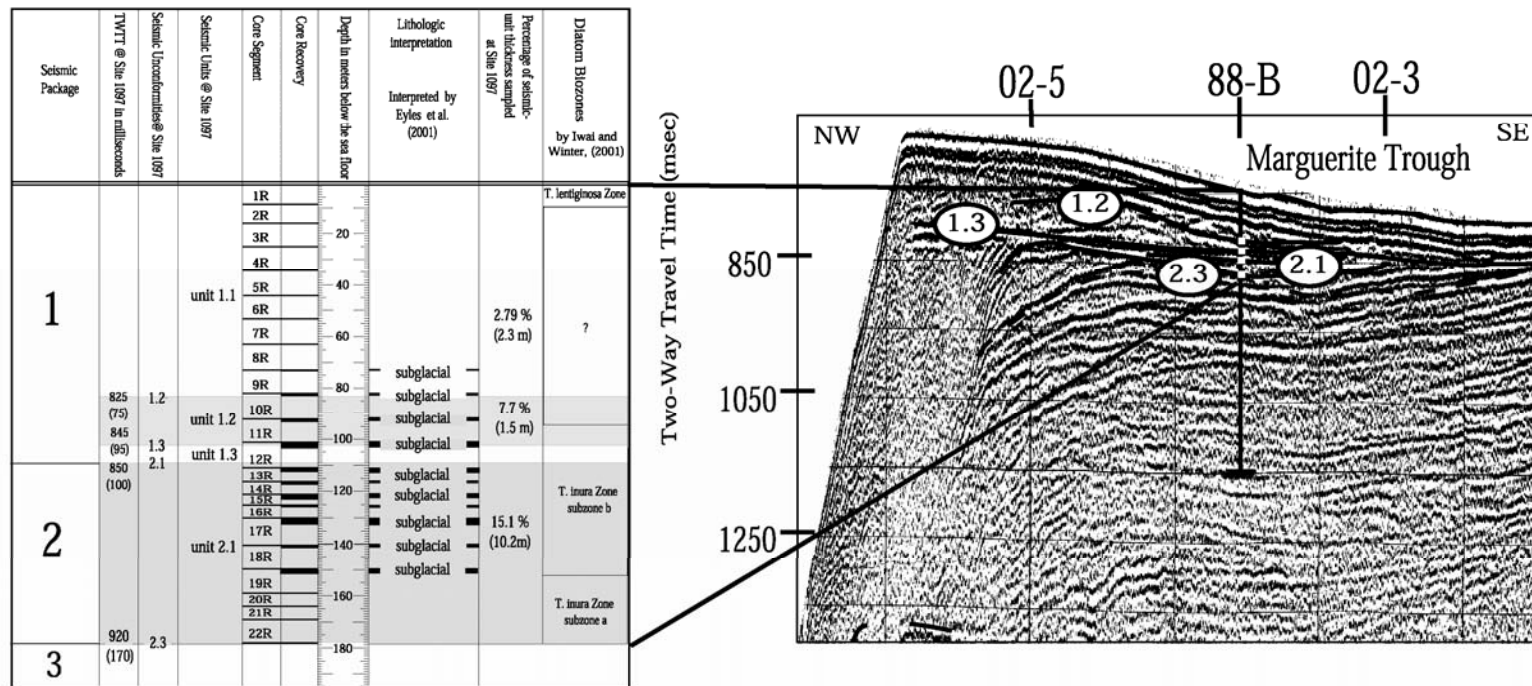


Figure 7: Line 88-4 passes through ODP site 1097 and Marguerite Trough. The line shows the location of ODP site 1097 and its location as it passes through packages one and two. Site 1097 samples units 1.1, 1.2 of package one and units 2.1 and 2.3 of package two. The base of package 2.3 is underlain by the top of package three at site 1097. These seismic unconformities and units have been projected into site 1097. The chart shows two-way travel time in milliseconds of the tops of the seismic units, core segment, core recovery, depth below sea floor in meters, lithologic interpretation of the ODP shipboard party, percentage of seismic unit sampled, and diatom occurrence. The top of unit 1.1 falls in the T. lentiginosa Zone. The lower half of unit 1.2 lies within the T. inura zone subzone b. Unit 1.3 and over half of unit 2.1 also lie in the T. inura zone subzone b. The lower part of unit 2.1, unconformity 2.3 and the top of package 3 lie within the T. inura zone subzone a. The above units have been interpreted by the ODP shipboard party as subglacial and are composed mainly of diamict.

Table 1: Position of seismic unconformities with respect to ODP site 1097.

Seismic Reflector	TWTT (msec bsf)	Depth (mbsf)	Core Segment	Diatom Zones at ODP Site 1097	Age (Ma) (Winter and Iwai, 2001)
Sea Floor (1.1)	0	0	1R	<i>T. lentiginosa</i>	
1.2	75	83	10R	?	
1.3	94	102	12R	<i>T. inura</i> subzone <i>b</i>	4.25-5.12
2.1	100	109	12R	<i>T. inura</i> subzone <i>a</i>	5.12-5.55
2.3	169	178	22R	<i>T. inura</i> subzone <i>a</i>	5.12-5.55

Seismic Unit 1.1 correlates with the *T. lentiginosa* - *A. ingens* zones and is approximately 80 meters thick. The time range for these zones is 0.64-1.85 Ma (Iwai and Winter, 2001) making Unit 1.1 Pleistocene in age. Seismic Unconformity 1.2 correlates to the base of the *T. lentiginosa* - *A. ingens* zones while most of Seismic Unit 1.2 lies within the *F. kerguelensis* Zone- *T. Kolbei* zone and is ~ 100 meters thick. The time range for these zones is 1 -2.4 Ma (Iwai and Winter, 2001) making unit 1.2 Late Pliocene in age. Seismic Unit 1.3 correlates to the top of the *T. vulnifica* zone and is ~ 60 meters thick at this location. The time range for this zone is 2.4-2.6 (Iwai and Winter, 2001) making Unit 1.3 Late Pliocene in age.

3.4 Mapping

A time structure map (Figure 9) of the top of Package 2 was constructed to get a general idea of how the morphology of the package compared with the modern bathymetry. The main features that both maps have in common are lobes 3 and 4.

Table 2: Table shows location of seismic unconformities in relation to ODP site 1103.

Seismic Reflection	TWTT (msec bsf)	Depth (mbsf)	Core Segment	Diatom Zones at ODP Site 1103	Age (Ma) (Iwai and Winter, 2001)
Sea Floor (1.1)	0	0	0	<i>T. lentiginosa</i> to <i>A. ingens</i> Zone	.64-1.85
1.2	65	80	9R	<i>T. lentiginosa</i> to <i>A. ingens</i>	.64-1.85
1.3	118	180	20R	<i>T. vulnifica</i>	2.4-2.6
Top of Package 3	240	240	26R		5.55-7.94

The expression of these features is an area of high elevation that gently slopes to a lower elevation. These packages are also positioned near the current shelf edge. A time structure map of the base of Package 2 (Figure 10) was also constructed to compare with the morphologies through various intervals. The base of Package 2 shows very little similarity to the present day morphology of the continental shelf. There is an indication of paleo-troughs at the base of Package 2.

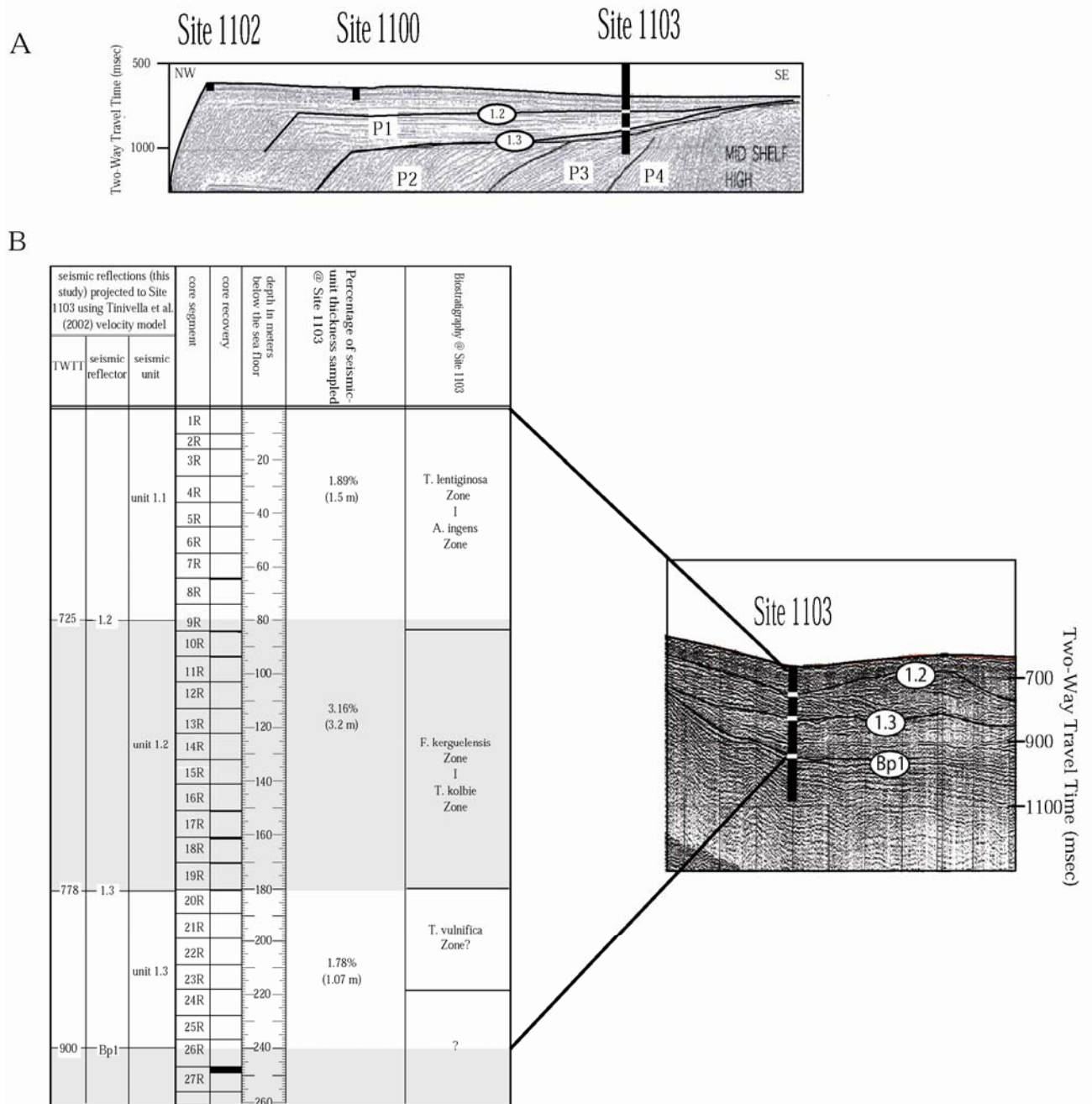


Figure 8: A) Seismic line I95-152 from ODP scientific results. This line passes through ODP sites 1102,1100,1103 and has been correlated to strike line 02-3. In this area, units 1.1,1.2,and 1.3 are present. Package two is absent at site 1103 and package three appears below package one. B) Seismic line 02-3 showing the position of ODP site 1103.

Unconformities 2.3, 2.4, 2.5 were mapped in order to detect paleo-trough morphology in unconformities that exhibited cross cutting relationships in seismic. The mapping of these unconformities (Figures 11,12, and 13) indicates the presence of paleo-troughs on the middle continental shelf. These troughs are only partial imaged in the maps due to cross cutting and erosion by subsequent advances of the ice sheet. The paleo-troughs are up dip of upper-slope progradation at the shelf edge.

An isopach map of Package 1 (Figure 16) was constructed to evaluate changes in package thickness over the study area. There are no large changes in the thickness of Package 1 over the study area. If significant progradation had occurred during Package 1 time, it would be expected that Package 1 would thicken toward the shelf edge near the lobes. Package 1 actually thins toward the shelf edge and there is no indication of large depo-centers at the shelf edge in Package 1. An isopach map of unit 1.1 (Figure 17), the upper most unit in Package 1, was mapped to compare any variations in thickness to the modern bathymetry. Unit 1.1 shows little variability in thickness (average thickness of 50 msec) over the area with small areas that thicken to ~100 msec.

Distribution maps (Figures 14 and 15 respectively) of the units in Packages 1 and 2 were created to get an idea of the location of units in these two packages. The units of Package 2 appear to be distributed into lobes bounded by areas in which Package 2 is absent. In contrast to Package 2, Package 1 is more wide spread with the exception of Unit 1.3 which is distributed in the southwestern and northeastern ends of the shelf.

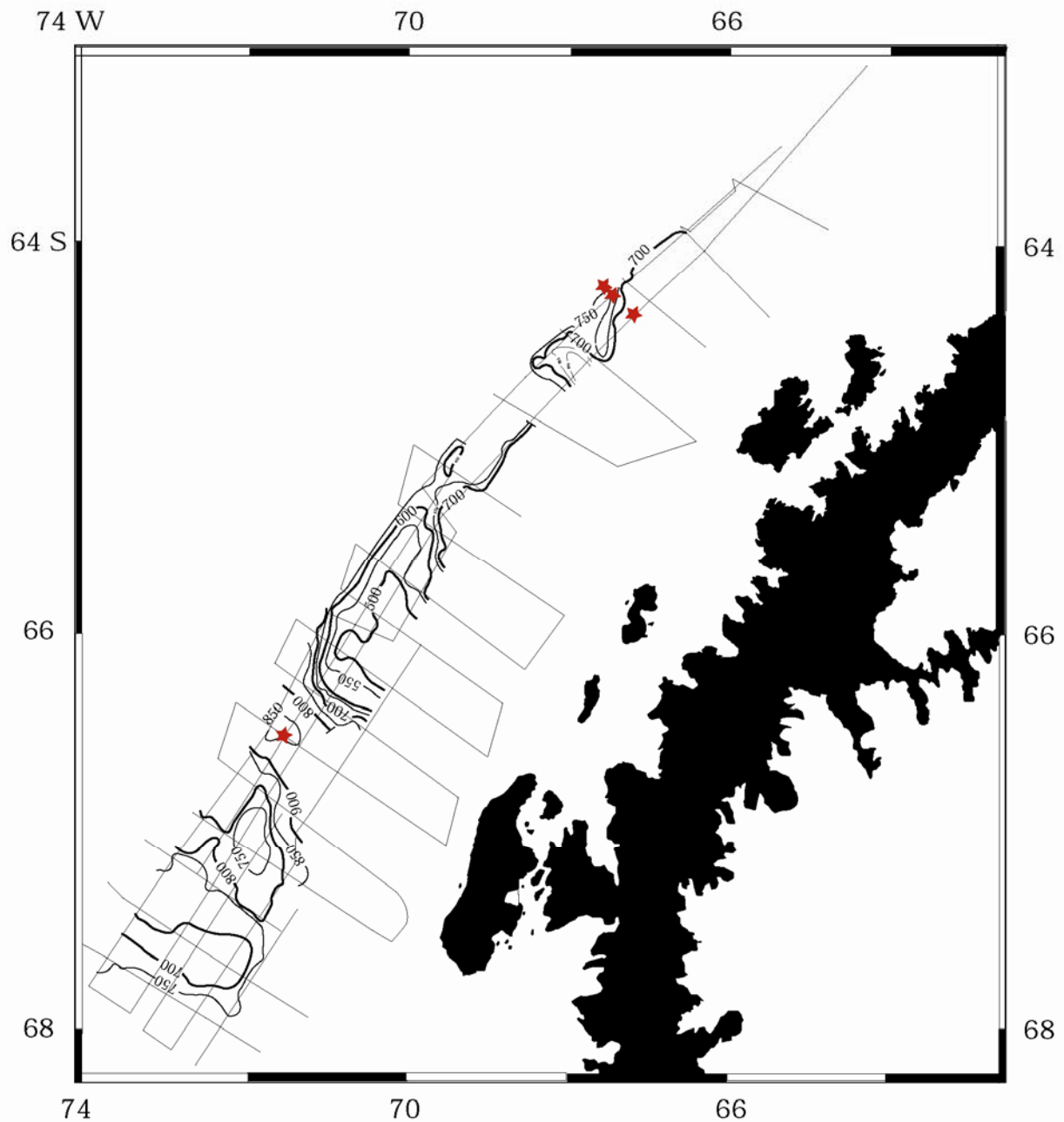


Figure 9: Time structure map of the top of Package 2. Data points for this map were measured from interpreted seismic lines in the data at 2.5 km intervals. The contour interval is 50 msec. The bold lines indicate contours at 100 msec intervals. If the morphology of the shelf has been created in the most recent glacial cycles, there should be a difference in the time structure map of the top of Package 2 and the modern bathymetry. In general the morphology of the sea floor mimics the structure of the top of Package 2. This would support the seismic evidence that shows a transition to aggradation by Unconformity 2.1.

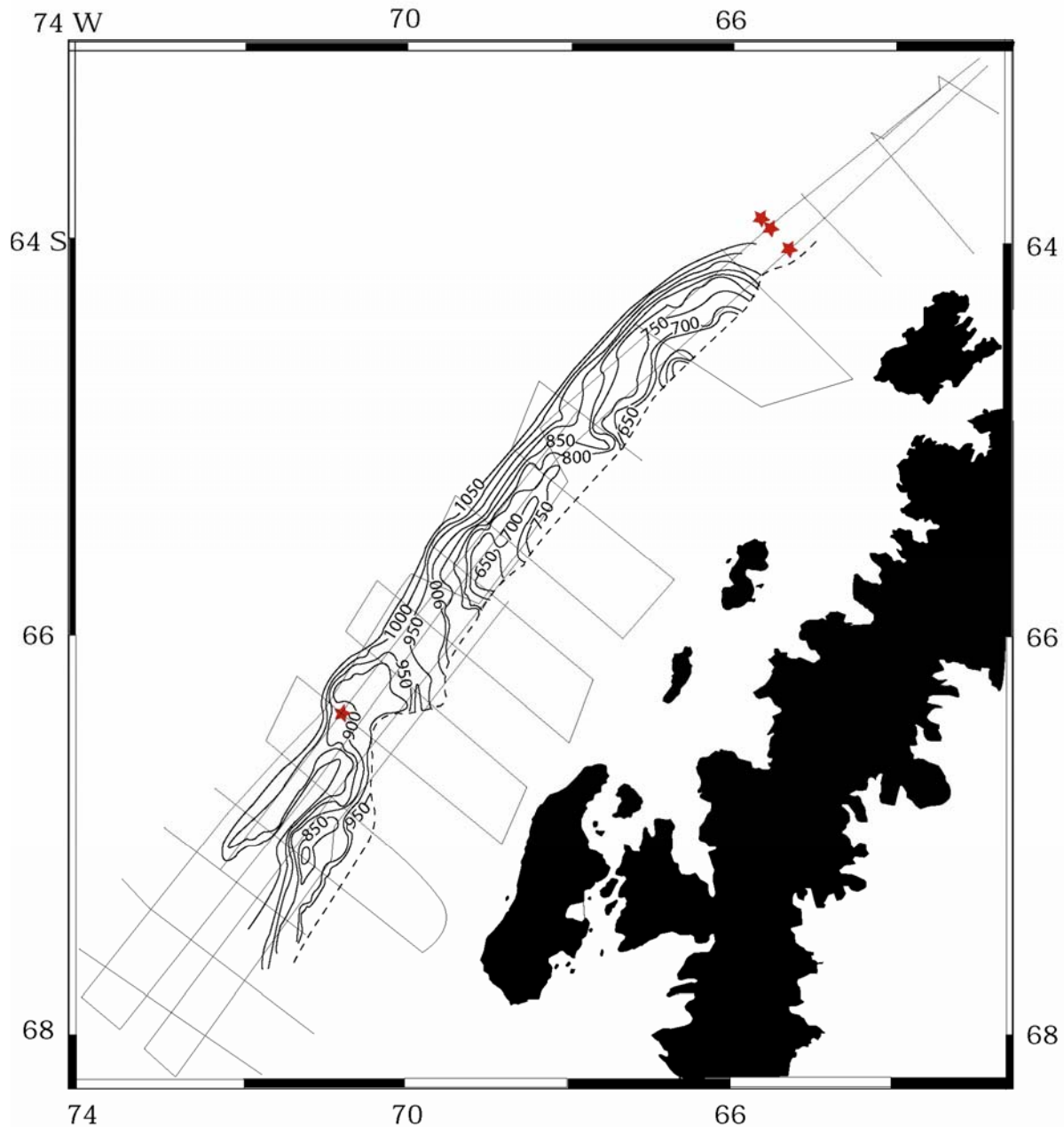


Figure 10 : A time-structure map of the base of Package 2. Contour interval is 50 msec. This map shows the morphology of the continental shelf before Package 2 time. The absence of the lobes formed during Package 2 is the most apparent feature of this map. The dotted line indicates the landward limit of the base of Package 2.

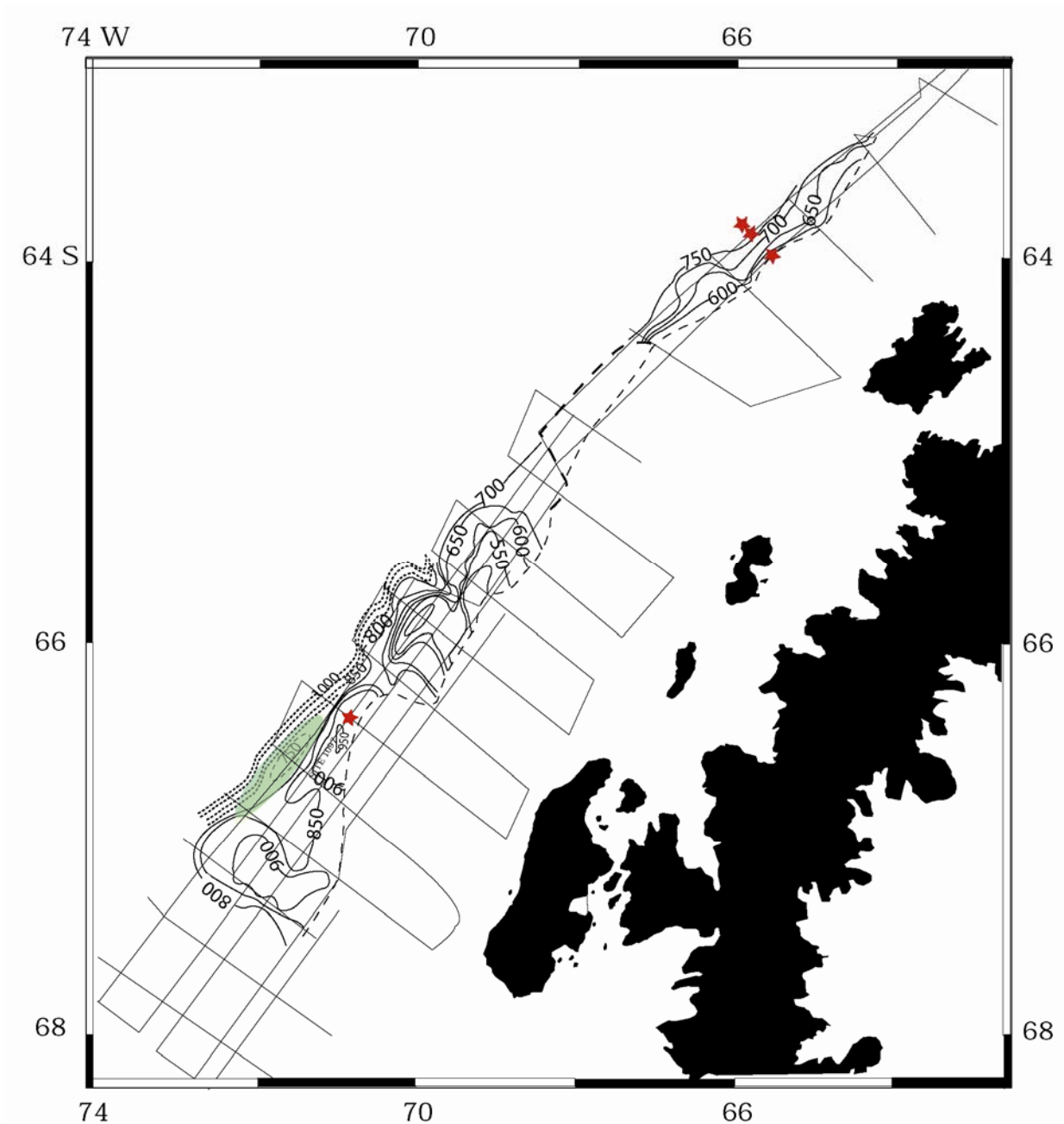


Figure 11: Time structure maps of interpreted glacial unconformity 2.3. Contour interval 50 milliseconds. Mapping of these unconformities show evidence of paleo-troughs and lobe development. Green oval indicates the position of seismic washout on line NBP02-05. This zone of seismic washout has been interpreted as upper slope progradation. The heavy dotted line indicates an area where unconformity 2.3 is absent. The light dotted line indicates the landward limit of unconformity 2.3.

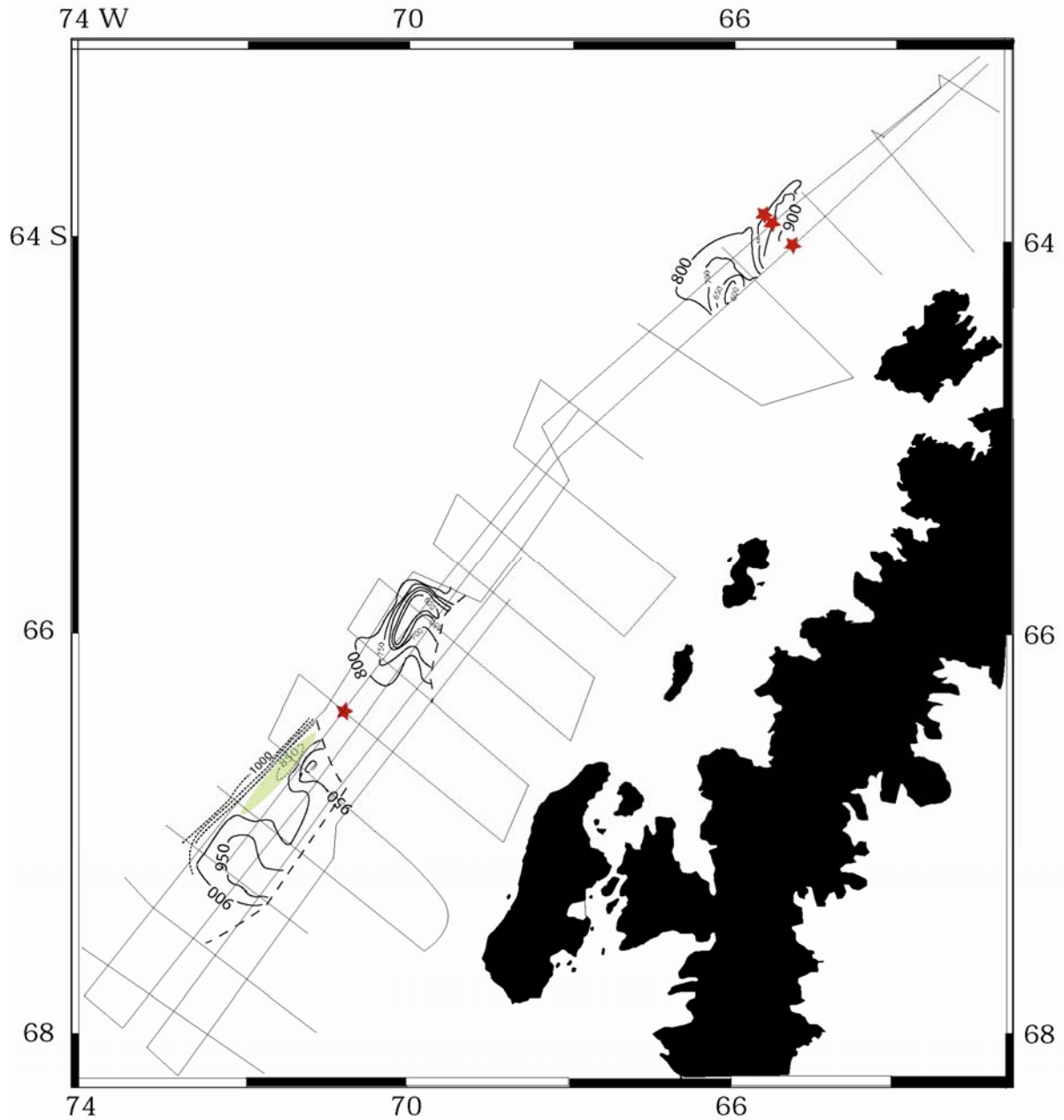


Figure 12: Time structure maps of interpreted glacial unconformity 2.4. Contour interval 50 milliseconds. Mapping of the unconformity shows evidence of paleo-troughs and lobe development. Green oval indicates the position of seismic washout on line NBP02-05. This zone of seismic washout has been interpreted as upper slope progradation.

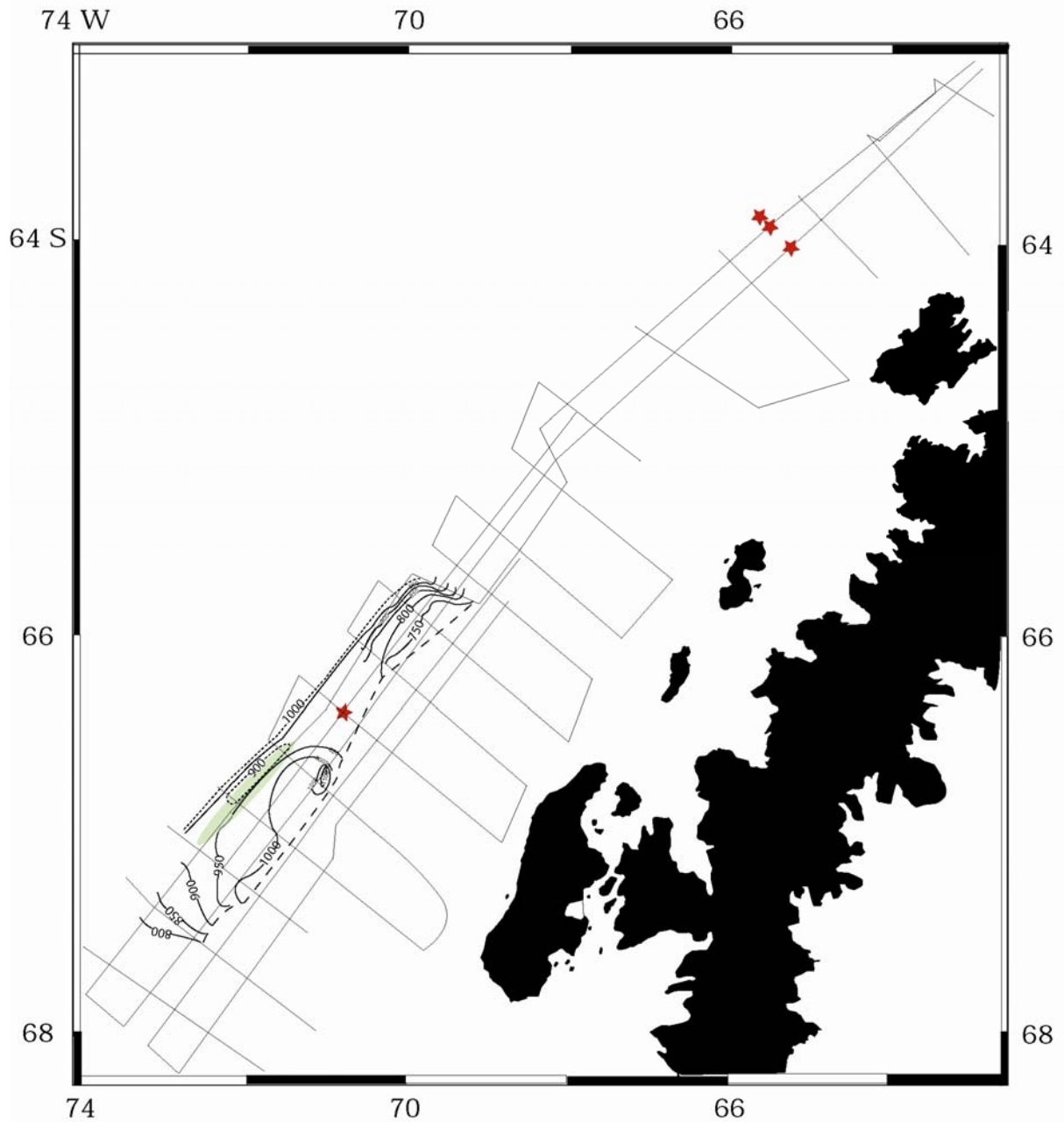


Figure 13: Time structure maps of interpreted glacial unconformity 2.5. Contour interval 50 milliseconds. Mapping of this unconformity shows evidence of paleo-troughs and lobe development. Green oval indicates the position of seismic washout on line NBP02-05. This zone of seismic washout has been interpreted as upper slope progradation.

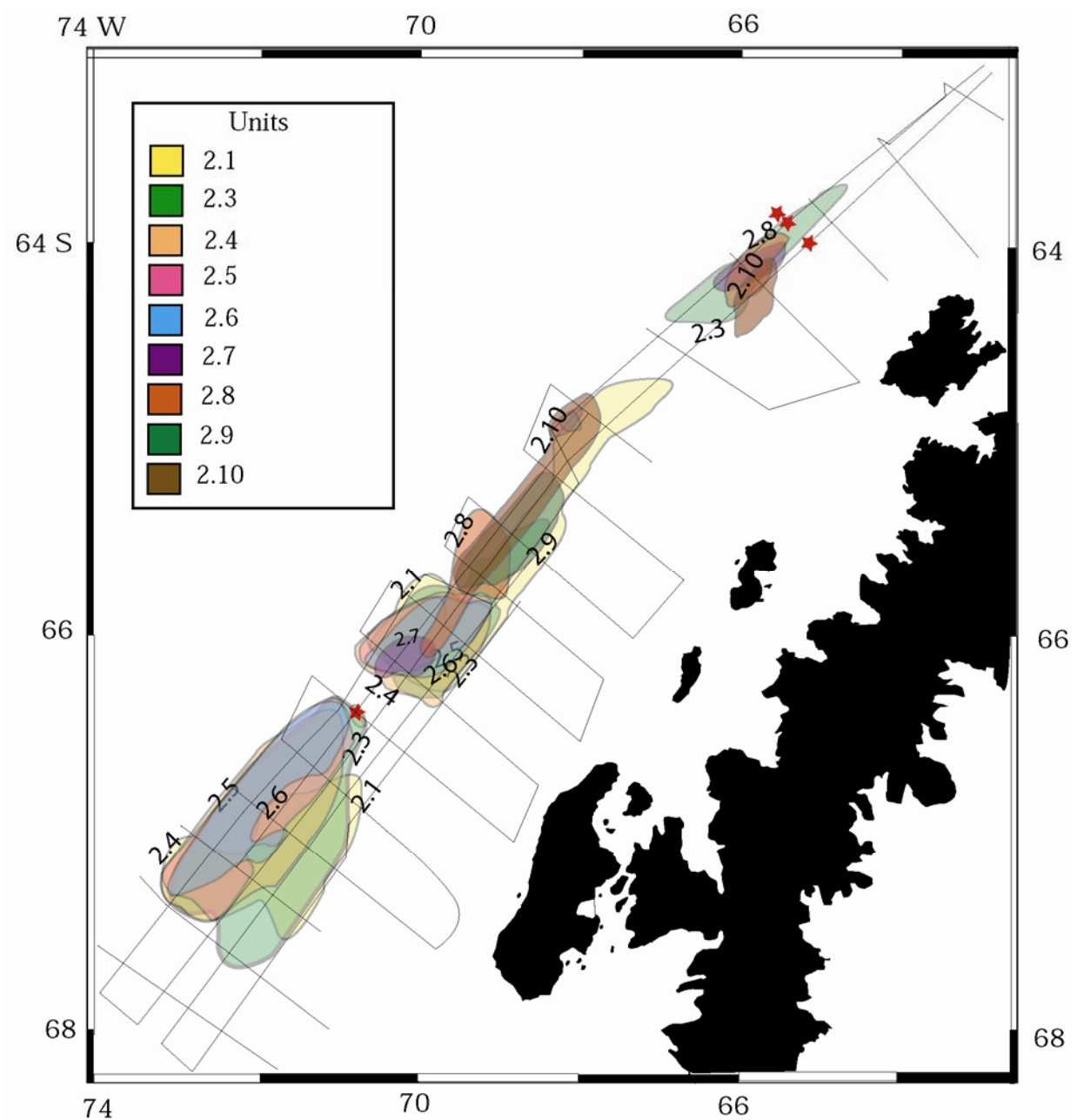


Figure 14 : Distribution map of Package 2 units on the continental shelf. Many units overly each other the absence of a unit is noted by the end of the black border around them.

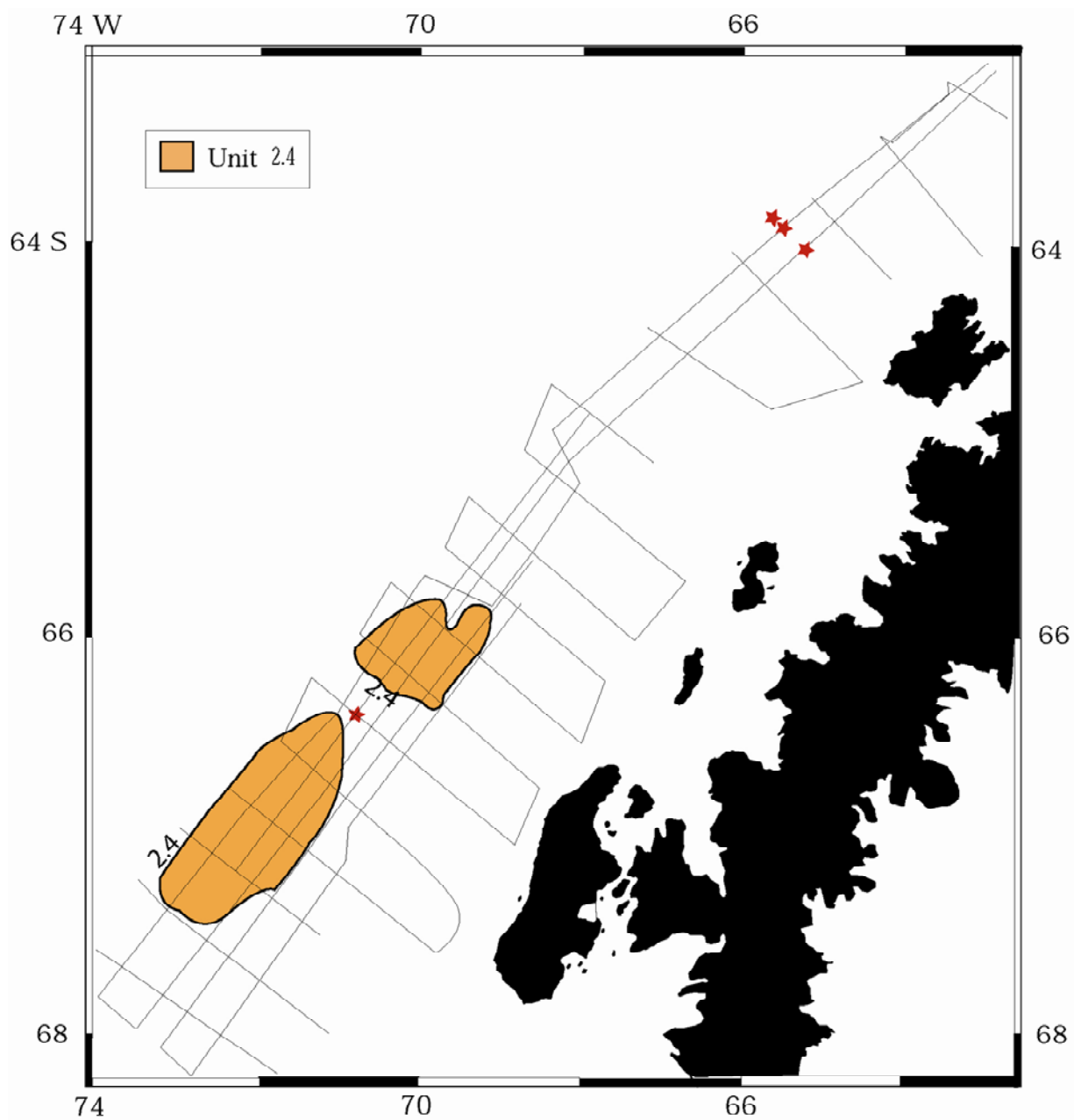


Figure 14a : Distribution map of unit 2.4 on the continental shelf. Absence of the unit is noted by the end of the black border around it.

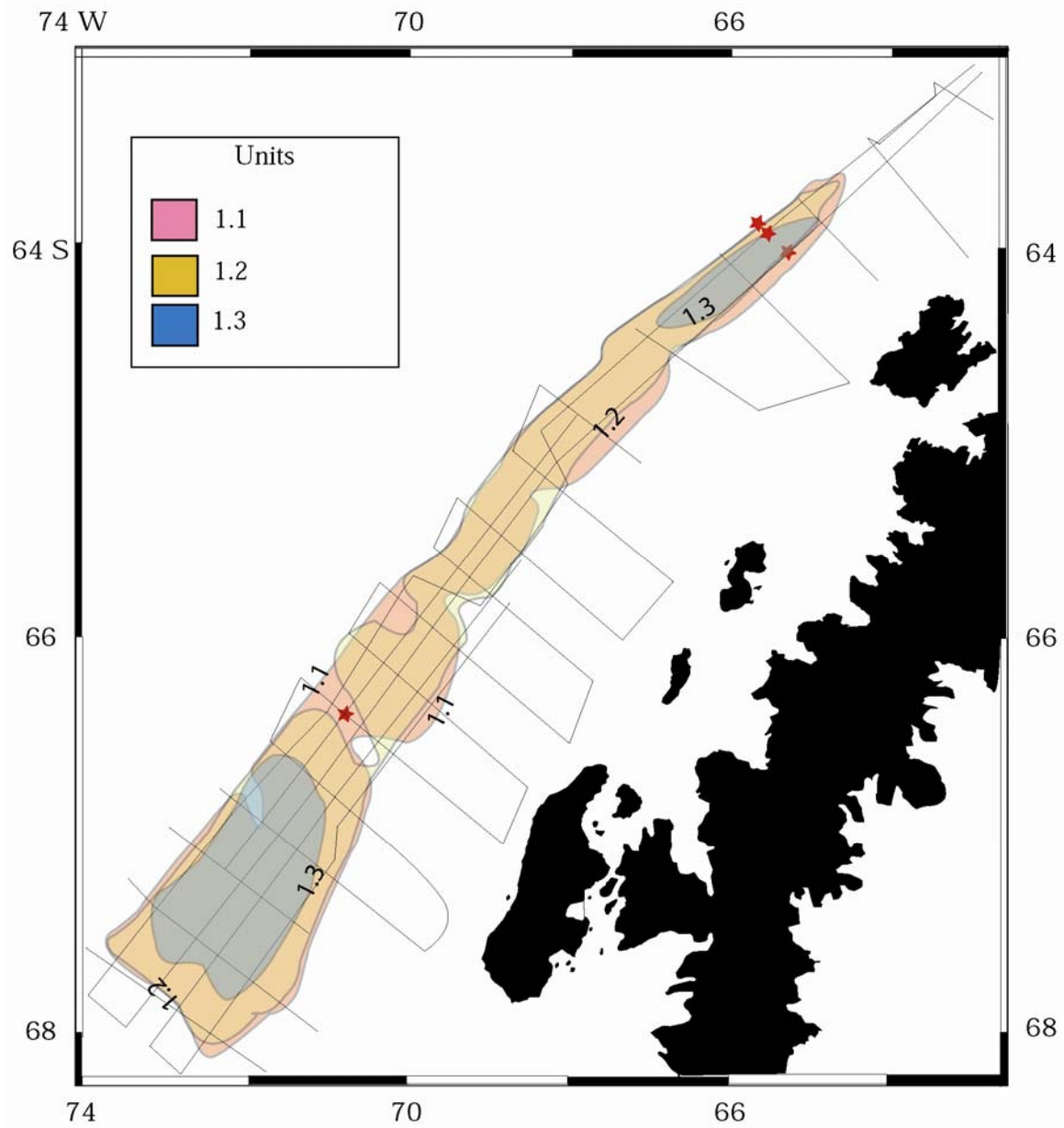


Figure 15: Distribution map of Package 1 units on the continental shelf. Many units overly each other the absence of a unit is noted by the end of the black border around them.

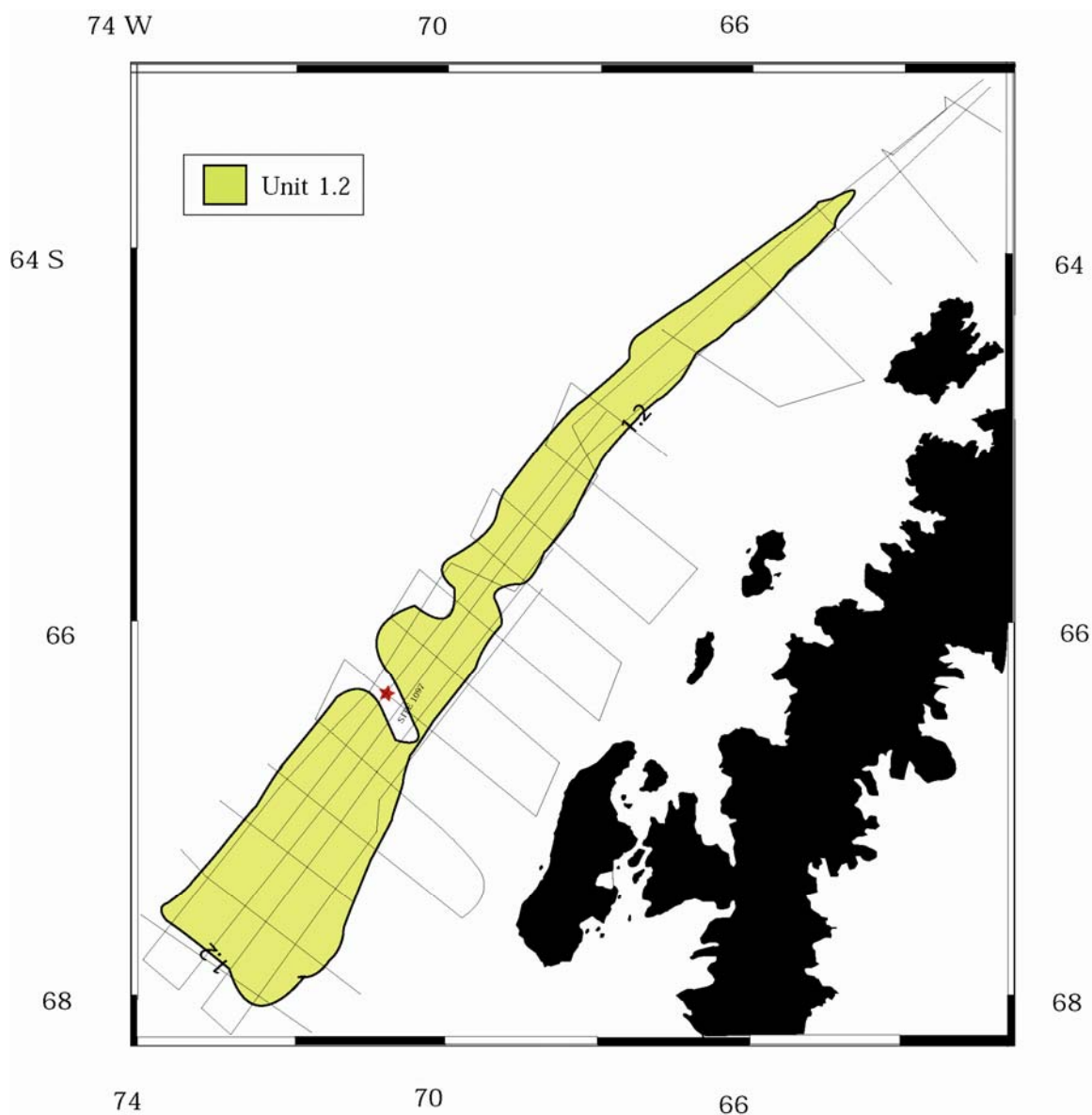


Figure 15a: Distribution map of unit 1.2 on the continental shelf. Many units overly each other, the absence of a unit is noted by the end of the black border around them.

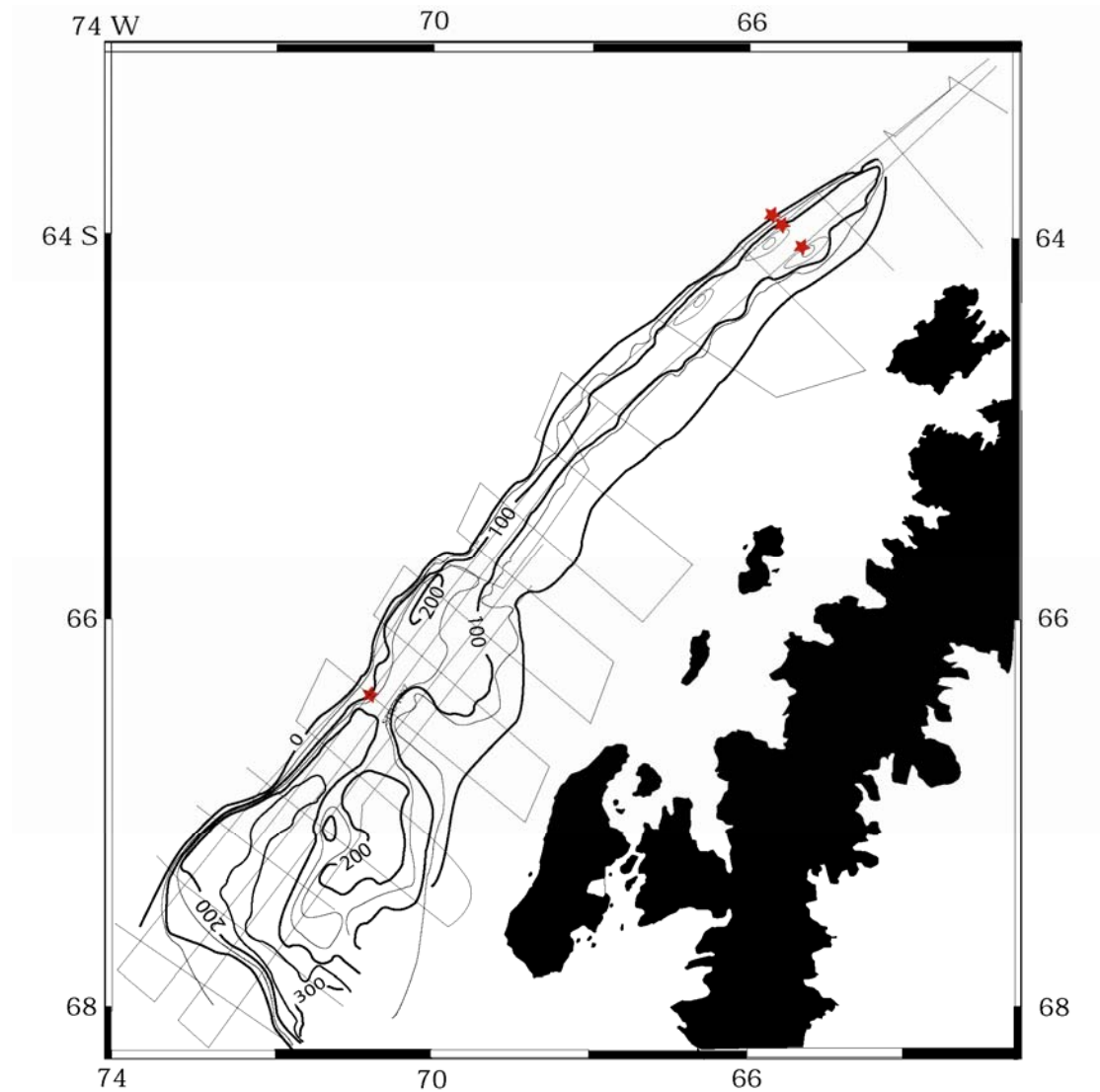


Figure 16: Isopach map of package one. Data points for this map were collected from interpreted seismic lines in the data set shown at 15 minute intervals. The contour interval is 50 msec. 100 msec contour interval is indicated by bold contours. If package one is mainly aggradational, there should be no large depo-centers at the shelf edge during package -1 time. This map shows no large depo-centers at the shelf edge and that is an indication of little progradation during this time.

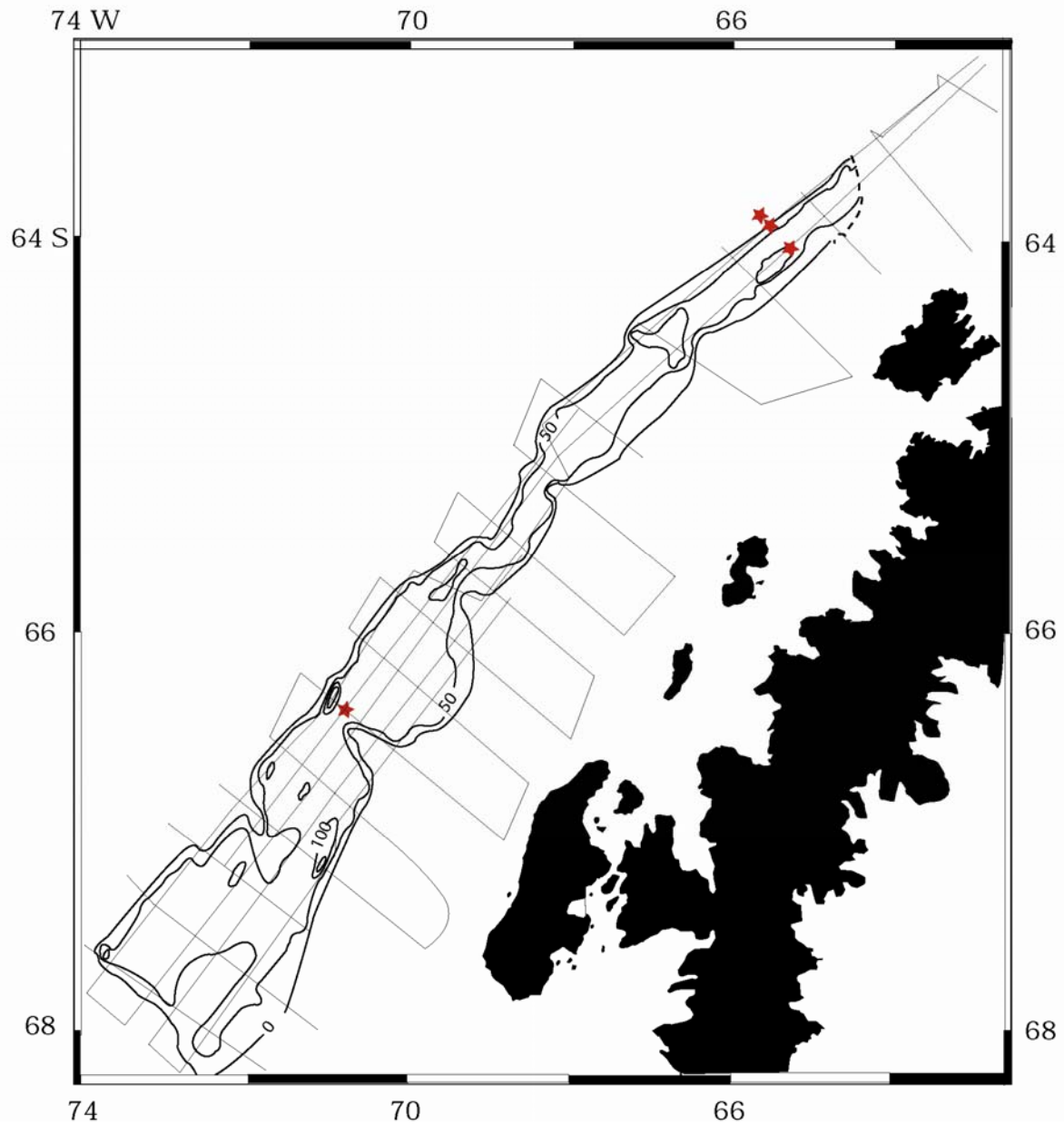


Figure 17: Isopach map of unit 1.1 with a contour interval of 50 msec. Thickness of unit 1.1 is constant over the study with scattered areas of thickness no more than 150 msec. This indicates a lack of lobe deposition and an aggradation of the Package 1 to match the sea floor bathymetry.

CHAPTER 4. DISCUSSION

The Rebesco et al. (1998) model relies on modern bathymetry to explain the evolution of the continental shelf. The subsurface data from seismic and ODP sites gives an alternative view of continental shelf evolution. An understanding of depositional processes and the timing of these processes is key to evaluating the evolution of the shelf.

4.1 Evidence of Trough Mouth Fans

Seismic surveys on the middle and outer continental shelf indicates major progradation of the margin early during Package-2 time. The modern bathymetry reflects this in the form of convex outward bulges at the shelf edge. These correspond to the lobes that would be formed by slow ice in the Rebesco et al. (1998) model. Interpretation of seismic data in this study gives a different view of the process that formed these lobes. When correlated to middle shelf seismic control, cross cutting relationships indicate paleo-troughs and evidence that ice streams occupied the area up dip of the upper-slope progradation. In addition, structure mapping of unconformities 2.3, 2.4, and 2.5 indicate the presence of paleo-troughs up dip of the large area of upper-slope progradation. This scenario constitutes trough-mouth fan development on the outer shelf/upper slope. From the standpoint of the Rebesco et al. (1998) model, these ice streams would be an area of bypass at the shelf edge/upper slope, instead of deposition. The distribution of Package 2 units appears to be focused in areas bounded by areas where Package 2 is absent. This could be an indication of the style of deposition. The occurrence of these units indicates deposition in the form of large depo-centers. This differs from the units of Package 1, which are widely distributed with few areas where the package is not present.

4.2 Evidence of a Relic Morphology – Transition from Progradation to Aggradation

Seismic also indicates a transition to aggradation in the upper part of Package 2. This aggradational pattern continues through Package 1 to the sea floor. The transition of the margin from progradational to aggradational is important to testing this model. Trough - mouth fan deposition during package-2 time is an interpretation that would explain the modern lobes that occur at the shelf edge. A time structure map of the base of Package 2 confirms the absence of the lobes before Package 2 time. After the deposition of the trough mouth fan, the transition to an aggradational setting would preserve the general morphology of the shelf. Lateral shifting of ice streams would create the present location of Marguerite Trough and other modern troughs on the continental shelf. This scenario would cause a blending of two morphologies on the continental shelf. A relic morphology formed by the progradational setting of Package 2, which would form the lobes expressed in the modern morphology (Figure 18), then a time (starting at ~5.12 Ma) when the margin was dominated by aggradation. Modern troughs were then formed to accompany the relic morphology. In essence, the morphology of the shelf must be evaluated as two separate systems, a modern component composed mainly of seafloor troughs and smaller scale sediment ridges and relic morphology composed of trough mouth fans (i.e. lobes).

A time structure map of the top of Package 2 confirms the existence of lobes 3 and 4 by the end of Package-2 time at (~5.12 Ma). These features are also coincident with the present shelf edge, which would indicate minimal progradation after lobe deposition (i.e. trough mouth fan). An isopach map of Package 1 indicates very little thickening of the

package at the shelf edge. There are also no large zones of thickness at the shelf edge, indicating no large depo-centers and in turn minimal progradation of the shelf edge.

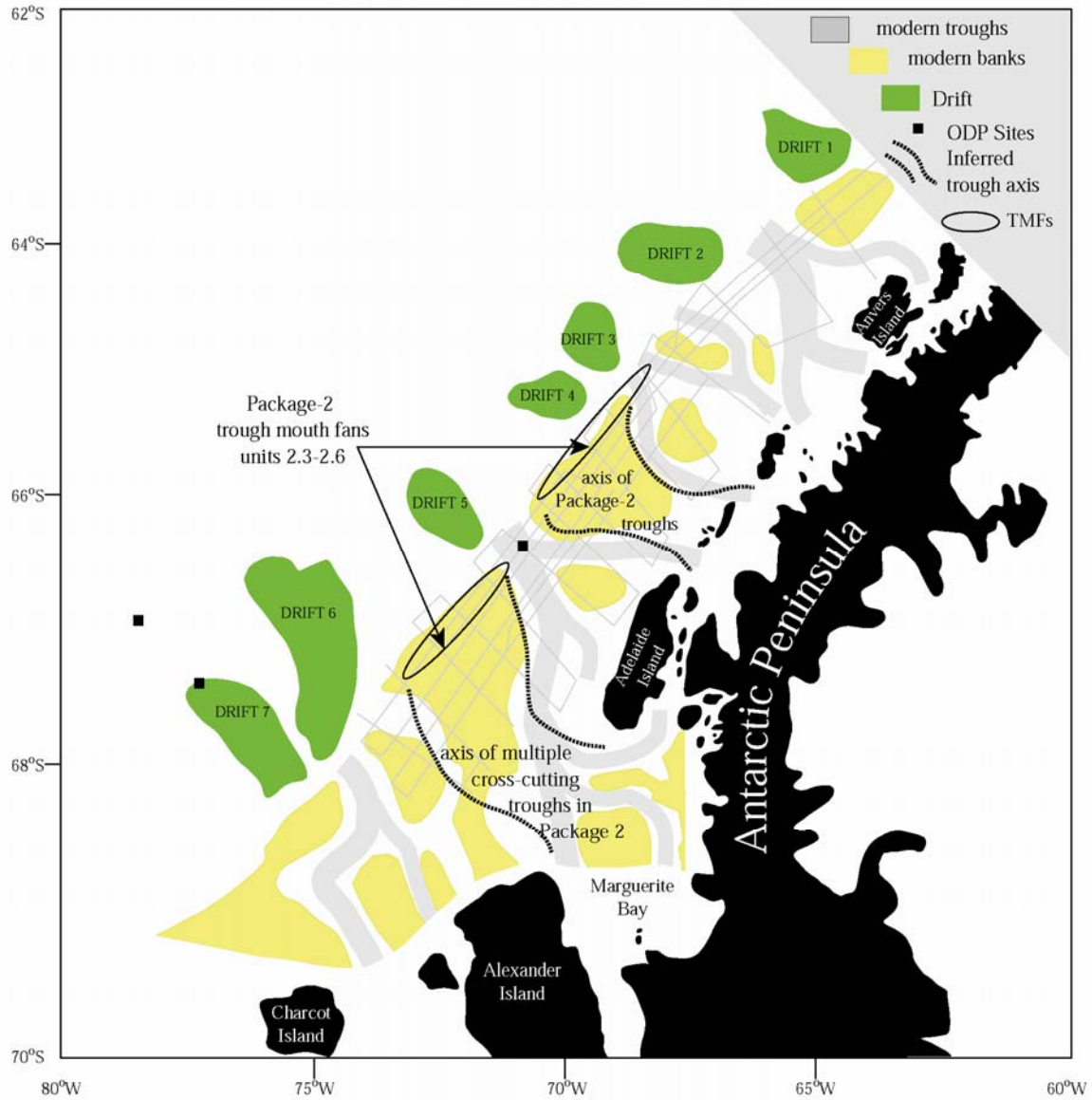


Figure 18: Paleo-reconstruction map of package -2 trough mouth fans and correlative package-2 paleo-troughs. Ovals indicate the location of trough-mouth fans and dotted lines indicate the axis of paleo-troughs (i.e. ice steams). These are overlain on the modern bathymetric lobes and troughs.

4.3 Timing Constrained from ODP Shelf Sites

Another key element to understanding the evolution of the continental shelf is the timing of the depositional processes. This can be resolved from biostratigraphic data obtained from ODP shelf drill sites. As a result, of correlation to ODP Site 1097 an age range of 5.12- 5.55 Ma can be assigned to the Unconformity 2.1, which is the top of Package 2. This would date the transition to aggradation during the latest Miocene to earliest Pliocene. This would further support the idea that the lobes (i.e. trough mouth fans) are relic features since they were deposited before Unconformity 2.1.

4.4 Possible Model for the Continental Shelf

A model (Figure 19) has been created that integrates the results of this study. The first stage of the model is an ice sheet advance with the development of ice streams early within Package 2 time. These ice streams erode troughs as the ice sheet advances. Sediment is transported subglacially and deposited at the mouth of the ice stream (trough mouth fan from Vorren et al. 1997). Subsequent ice sheet advances aggrade the shelf and ice streams form new troughs but do not deposit new depocenters. The depocenters formed during package 2 time are aggraded and the morphology is preserved.

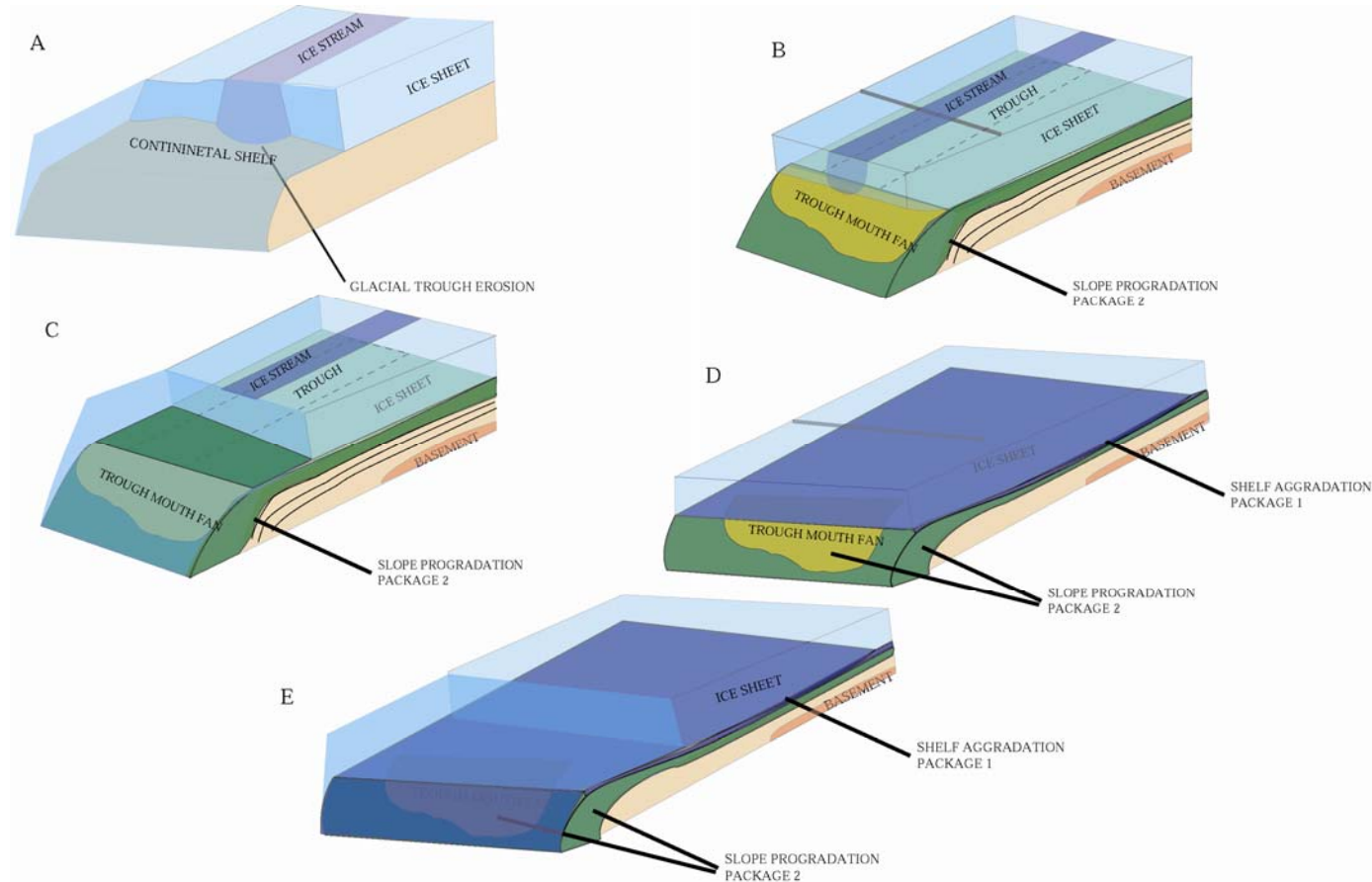


Figure 19: Model of continental shelf evolution derived from the data of this study. Stage one (A) of this model shows an ice sheet advance with ice stream development on the continental shelf. A trough is eroded into the continental shelf and sediment is transported subglacially. The second stage (B) is the deposition of a trough- mouth fan as sediments are fed to the upper slope. The green section is upper slope progradation. The third is the retreat of the ice sheet to the inner shelf. The fourth (D) stage is a subsequent ice sheet advance that aggrades the continental shelf. This sediment is indicated by the blue section. The final stage (E) is the resulting continental shelf configuration.

CHAPTER 5. CONCLUSIONS

This study has confirmed the presence of former ice streams (paleo-troughs) and correlative upper slope progradation. This evidence indicates the presence of trough-mouth fans, which indicates a flaw in the Rebesco et al. (1998) model. There was limited bypass during Package-2 time and deposition of large fans at the mouth of troughs. This has shaped the morphology of the modern shelf. The age control provided by diatom biozones at the ODP sites supports the idea of progradation of the margin during the latest Miocene to earliest Pliocene with a transition to aggradation during the Pliocene (?) which preserved the relic morphology of the continental shelf. The transition occurred at ~2.5 Ma and occurs after the deposition of unit 2.3 and before the deposition of unit 2.1.

REFERENCES

- Alley, R. B., D. D. Blankenship, S. T. Rooney, and C. R. Bentley (1989), Sedimentation beneath ice shelves; the view from ice stream B, *Mar. Geol.*, 85(2-4), 101-120.
- Anderson, J. B. (1999), *Antarctic Marine Geology*, 289 pp., Cambridge University Press, Cambridge.
- Barker, P. F., and A. Camerlenghi (2001), Synthesis of Leg 178 results: glacial history of the Antarctic Peninsula from Pacific margin sediments, in *Proc. ODP, Sci. Results*, vol. 178, edited by P. F. Barker, A. Camerlenghi, G. D. Acton, and A. T. S. Ramsay, [CD-ROM]. Available from Ocean Drilling Program, Texas A&M University, College Station, Texas 77845-9547, USA.
- Barker, P. F., and A. K., Cooper (Eds.) (1997), *Geology and Seismic Stratigraphy of the Antarctic Margin (Pt. 2)*, *Antarct. Res. Ser.*, vol. 71, 187 pp., AGU, Washington, D.C.
- Bart, P. J., and J. B. Anderson (1995), Seismic record of glacial events affecting the Pacific margin of the northwestern Antarctic Peninsula, in *Geology and Seismic Stratigraphy of the Antarctic Margin*, *Antarct. Res. Ser.*, vol. 68, edited by A. K. Cooper, P. R. Barker, and G. Brancolini, pp. 75-95, AGU, Washington, D.C.
- Bart, P. J., and J. B. Anderson (1996), Seismic expression of depositional sequences associated with expansion and contraction of ice sheets on the northwestern Antarctic Peninsula continental shelf, in *Geology of Siliciclastic Shelf Sea*, *Geol. Soc. Spec. Pub.*, vol. 117, edited by M. De Batist and P. Jacobs, pp. 171-186, The Geological Society, London.
- Canals, M., R. Urgueles, and A. M. Calafat (2000), Deep sea-floor evidence of past ice streams off the Antarctic Peninsula, *Geology*, 28, 31-34.
- Denton, G. H., M. L. Prentice, and H. Burckle (1991), Cainozoic history of the Antarctic Ice Sheet, in *The Geology of Antarctica*, edited by R. J. Tingey, pp. 365-463, Clarendon Press, Oxford
- Dowdeswell, J.A., C. Ó Cofaigh, and C. J. Pudsey (2004), Thickness and extent of the subglacial till layer beneath an Antarctic paleo-ice stream, *Geology*, 32, 13-16.
- Eyles, N., J. Daniels, L. E. Osterman, and N. Januszczak (2001), Ocean Drilling Program Leg 178 (Antarctic Peninsula): sedimentology of glacially influenced continental margin topsets and foresets, *Mar. Geol.*, 178, 135-156.
- Iwai, M., and D. Winter (2001), Data Report: Taxonomic Notes on Neogene Diatoms from the western Antarctic Peninsula: Ocean Drilling Program Leg 178, in *Proc. ODP, Sci. Results*, vol. 178, edited by P. F.

Barker, A. Camerlenghi, G. D. Acton, and A. T. S. Ramsay, [CD-ROM]. Available from Ocean Drilling Program, Texas A&M University, College Station, Texas 77845-9547, USA.

Larter, R. D., and P. F. Barker (1989), Seismic stratigraphy of the Antarctic Peninsula Pacific margin: a record of Pliocene-Pleistocene ice volume and paleoclimate, *Geology*, *17*, 731-734.

Larter, R.D., and A.P. Cunningham (1993), The depositional pattern and distribution of glacial-interglacial sequences on the Antarctic Peninsula Pacific Margin, *Mar. Geol.*, *109*, 203-219.

Larter, R. D., and L. E. Vanneste (1995), Relict subglacial deltas on the Antarctic Peninsula outer shelf, *Geology*, *23*(1), 33-36.

Moerz, T., R. Laronga, C. Lauer-Leredde, C. Escutia, and T. C. W. Wolf-Welling (2001), Composite velocity profile of shelf Site 1103 (ODP Leg 178, western Antarctic Peninsula), in *Proc. ODP, Sci. Results*, vol. 178, edited by P. F. Barker, A. Camerlenghi, G. D. Acton, and A. T. S. Ramsay, [CD-ROM], available from Ocean Drilling Program, Texas A&M University, College Station, Texas 77845-9547, USA.

Pope, P. G., and J. B. Anderson (1992), Late Quaternary glacial history of the northern Antarctic Peninsula's western continental shelf: evidence from the marine record, in *Contributions to Antarctic Research III, Antarct. Res. Ser. AGU*, vol. 57, edited by D. H. Elliot, pp. 63-91, AGU, Washington, D.C.

Pudsey, C.J., P.F. Barker, and R.D. Larter (1994), Ice sheet retreat from the Antarctic Peninsula shelf, *Cont. Shelf Res.*, *14*, 1647-1675.

Rebesco, M., A. Camerlenghi, L. DeSantis, E.W. Domack, and M.E. Kirby (1998), Seismic stratigraphy of Palmer Deep: a fault-bounded Late Quaternary sediment trap on the inner continental shelf, Antarctic Peninsula Pacific margin, *Mar. Geol.*, *151*, 89-110.

Rebesco, M., A. Camerlenghi, C. Zanolla, Bathymetry and morphogenesis of the continental margin west of the Antarctic Peninsula. *Terr Antarctica* *5*(4) (1998) 715-725.

Shipboard Scientific Party (1999), Leg 178 summary, in *Proc. ODP, Initial Reports*, vol. 178, edited by P. F. Barker, A. Camerlenghi, and G. D. Acton, [CD-ROM]. Available from Ocean Drilling Program, Texas A&M University, College Station, Texas 77845-9547, USA.

Sloan, B. J, L. Lawver, J. Anderson (1995), Seismic stratigraphy of the Larsen Basin, eastern Antarctic Peninsula, in *Geology and Seismic Stratigraphy of the Antarctic Margin, Antarct. Res. Ser.*, vol. 68, edited by A. K. Cooper, P. R. Barker, and G. Brancolini, pp. 59-74, AGU, Washington, D.C.

Stokes, C and C. Clark , Palaeo-ice streams, *Quaternary Science Reviews* , July 2001, Vol. 20, Issue 13, pp. 1437-1457.

Tinivella, U., A. Camerlenghi and M. Rebesco (2001), Data report: Seismic velocity analysis on the continental shelf transect, ODP Leg 178, Antarctic Peninsula, in *Proc. ODP, Sci. Results*, vol. 178, edited by P. F. Barker, A. Camerlenghi, G. D. Acton, and A. T. S. Ramsay, [CD-ROM], available from Ocean Drilling Program, Texas A&M University, College Station, Texas 77845-9547, USA.

.Vorren, Tore O. and J.S. Laberg, Trough mouth fans; palaeoclimate and ice-sheet monitors. *Quaternary Science Reviews*, 1997, Vol. 16, Issue 8, pp. 865-881.

Winter, D. and M. Iwai (2001), Neogene Diatom Biostratigraphy, Antarctic Peninsula Pacific Margin, ODP Leg 178 Rise Sites, in *Proc. ODP, Sci. Results*, vol. 178, edited by P. F. Barker, A. Camerlenghi, G. D. Acton, and A. T. S. Ramsay, [CD-ROM]. Available from Ocean Drilling Program, Texas A&M University, College Station, Texas 77845-9547, USA.

APPENDIX A. TIME – DEPTH CONVERSIONS FOR ODP SITES

I used a detailed two-way-travel time (TWTT) - depth conversion table created by Dr. Philip Bart for Site 1097 using the 42 measurements of P-wave-velocity from a Hamilton-Frame sensor pair, PWS3 for core recovered at Site 1097 (Shipboard Scientific Party, 1999). At Site 1103, I used TWTT-depth conversions for the Packages 1 and 2 glacial unconformities by utilizing the Tinivella et al. (2001) velocity estimates for this site.

Summary table of time to depth conversions for unconformities sampled at ODP Site 1103.

A.) Seismic reflection (this study)	B.) TWTT-D conversion via Tinivella et al. (2001) velocity model		
	TWTT (msec bss)	TWTT (msec bsf)	Depth (mbsf)
Seafloor	660	0	0
Unc. 1.2	725	65	80
Unc. 1.3	950	118	180
Base of Package one	900	240	240

Summary table of time to depth conversions for unconformities sampled at ODP Site 1097.

A.) Seismic reflection (this study)	B.) TWTT-D conversion via velocity model interpolation from ODP Site 1097 Hamilton Sensor Pair Velocities		
	TWTT (msec bss)	TWTT (msec bsf)	Depth (mbsf)
Seafloor	775	0	0
Unc. 1.2	825	75	83
Unc. 1.3	845	95	102
Unc. 2.1	850	100	109
Unc. 2.3	920	170	178

Seismic travel time-depth conversions at Site 1097

Site 1097 Interpolation Table

Depth = meters below sea floor, depth to the top of the bed of interest

Thick. = Thickness in meters of the bed of interest

Velocity = meters per second, velocity through bed of interest

TWTT= milliseconds, two-way-travel time to the top of the bed of interest (including time from overlying beds)

TWTB= milliseconds, two-way-travel time to the bottom of the bed of interest (including time from overlying beds)

Depth (mbsf)	Thick. (m)	Vel. (m/s)	TWTT(ms)	TWTB(ms)
0	1	2000	0	1
1	1	2005.511641	1	1.997251753
2	1	2011.023281	1.997251753	2.991770325
3	1	2016.534922	2.991770325	3.983570654
4	1	2022.046562	3.983570654	4.972667561
5	1	2027.558203	4.972667561	5.959075743
6	1	2033.069843	5.959075743	6.942809778
7	1	2038.581484	6.942809778	7.923884126
8	1	2044.093124	7.923884126	8.90231313
9	1	2049.604765	8.90231313	9.878111017
10	1	2055.116405	9.878111017	10.8512919
11	1	2060.628046	10.8512919	11.82186978
12	1	2066.139686	11.82186978	12.78985854
13	1	2071.651327	12.78985854	13.75527197
14	1	2077.162967	13.75527197	14.71812372
15	1	2082.674608	14.71812372	15.67842736
16	1	2088.186249	15.67842736	16.63619633
17	1	2093.69789	16.63619633	17.59144399
18	1	2099.209531	17.59144399	18.54418356
19	1	2104.721172	18.54418356	19.4944282
20	1	2110.232813	19.4944282	20.44219092
21	1	2115.744454	20.44219092	21.38748467
22	1	2121.256095	21.38748467	22.33032227
23	1	2126.767736	22.33032227	23.27071645
24	1	2132.279377	23.27071645	24.20867985
25	1	2137.791018	24.20867985	25.14422499
26	1	2143.302659	25.14422499	26.07736432
27	1	2148.8143	26.07736432	27.00811017
28	1	2154.325941	27.00811017	27.9364748

29	1	2159.837582	27.9364748	28.86247036
30	1	2165.349223	28.86247036	29.78610891
31	1	2170.860864	29.78610891	30.70740241
32	1	2176.372505	30.70740241	31.62636274
33	1	2181.884146	31.62636274	32.5430017
34	1	2187.395787	32.5430017	33.45733098
35	1	2192.907428	33.45733098	34.36936218
36	1	2198.419069	34.36936218	35.27910685
37	1	2203.93071	35.27910685	36.18657639
38	1	2209.442351	36.18657639	37.09178219
39	1	2214.953992	37.09178219	37.99473548
40	1	2220.465633	37.99473548	38.89544747
41	1	2225.977274	38.89544747	39.79392924
42	1	2231.488915	39.79392924	40.69019182
43	1	2237.000556	40.69019182	41.58424614
44	1	2242.512197	41.58424614	42.47610306
45	1	2248.023838	42.47610306	43.36577335
46	1	2253.535479	43.36577335	44
47	1	2259.04712	44.2532677	45.13859674
48	1	2264.558761	45.13859674	46.021771
49	1	2270.070402	46.021771	46.90280095
50	1	2275.582043	46.90280095	47.78169698
51	1	2281.093684	47.78169698	48.65846939
52	1	2286.605325	48.65846939	49.53312843
53	1	2292.116966	49.53312843	50.40568426
54	1	2297.628607	50.40568426	51.27614696
55	1	2303.140248	51.27614696	52.14452657
56	1	2308.651889	52.14452657	53.01083301
57	1	2314.16353	53.01083301	53.87507618
58	1	2319.675171	53.87507618	54.73726587
59	1	2325.186812	54.73726587	55.59741182
60	1	2330.698453	55.59741182	56.45552369
61	1	2336.210094	56.45552369	57.31161109
62	1	2341.721735	57.31161109	58.16568354
63	1	2347.233376	58.16568354	59.01775051
64	1	2352.745017	59.01775051	59.86782138
65	1	2358.256658	59.86782138	60.7159055
66	1	2363.768299	60.7159055	61.56201213
67	1	2369.27994	61.56201213	62.40615046
68	1	2374.791581	62.40615046	63.24832964
69	1	2380.303222	63.24832964	64.08855873
70	1	2385.814863	64.08855873	64.92684676
71	1	2391.326504	64.92684676	65.76320265
72	1	2396.838145	65.76320265	66.59763531
73	1	2402.349786	66.59763531	67.43015355
74	1	2407.861427	67.43015355	68.26076615
75	1	2413.373068	68.26076615	69.08948179
76	1	2418.884709	69.08948179	69.91630914
77	1	2424.39635	69.91630914	70.74125677
78	1	2429.907991	70.74125677	71.56433321

79	1	2435.419632	71.56433321	72.38554693
80	1	2440.931273	72.38554693	73.20490635
81	1	2446.442914	73.20490635	74.02241982
82	1	2451.954555	74.02241982	74.83809563
82.9	0.9	2456.915	74.83809563	75.57072171
83	0.1	2451.414156	75.57072171	75.65230726
84	1	2396.405716	75.65230726	76.48689048
85	1	2341.397276	76.48689048	77.34108128
86	1	2286.388835	77.34108128	78.21582313
87	1	2231.380395	78.21582313	79.11212929
88	1	2176.371955	79.11212929	80.03108985
89	1	2121.363515	80.03108985	80.97387971
90	1	2066.355075	80.97387971	81.94176757
91	1	2011.346635	81.94176757	82.93612626
92	1	1956.338194	82.93612626	83.95844439
92.26	0.26	1942.036	83.95844439	84.22620462
93	0.74	1934.127	84.22620462	84.99140771
94	1	1923.439	84.99140771	86.03121194
95	1	1912.751	86.03121194	87.07682634
96	1	1902.063	87.07682634	88.12831623
97	1	1891.375	88.12831623	89.18574799
98	1	1880.687	89.18574799	90.24918917
99	1	1869.999	90.24918917	91.31870846
100	1	1859.311	91.31870846	92.39437573
101	1	1848.623	92.39437573	93.47626209
102	1	1837.935	93.47626209	94.56443985
102.816	0.816	1829.214	94.56443985	95.45662633
103	0.184	1838	95.45662633	95.65680733
104	1	1887.915	95.65680733	96.71617706
105	1	1937.494	96.71617706	97.74843832
106	1	1987.073	97.74843832	98.75494387
107	1	2036.652	98.75494387	99.73694767
108	1	2086.231	99.73694767	100.6956143
109	1	2135.81	100.6956143	101.6320272
110	1	2185.389	101.6320272	102.547196
111	1	2234.968	102.547196	103.4420634
111.861	0.861	2277.661	103.4420634	104.1981022
112	0.139	2279.527214	105.085862	105.2078171
113	1	2292.953214	105.2078171	106.0800547
114	1	2306.379214	106.0800547	106.9472148
115	1	2319.805214	106.9472148	107.8093561
116	1	2333.231214	107.8093561	108.6665365
116.271	0.271	2336.868	108.6665365	108.8984709
117	0.729	2326.65	109.653891	110.2805431
118	1	2312.634	110.2805431	111.1453578
119	1	2298.618	111.1453578	112.0154458
120	1	2284.602	112.0154458	112.8908718
121	1	2270	112.8908718	113.7717017
121.93	0.93	2257.551	113.7717017	114.5956034
122	0.07	2256.415	114.828556	114.8906013

123	1	2240.182	114.8906013	115.7833859
124	1	2223.949	115.7833859	116.6826871
125	1	2207.716	116.6826871	117.5886007
125.8	0.8	2194.728	117.5886007	118.3176205
126	0.2	2194.184	118.3176205	118.4999501
127	1	2191.464	118.4999501	119.412582
128	1	2188.744	119.412582	120.3263481
129	1	2186.024	120.3263481	121.2412511
130	1	2183.304	121.2412511	122.157294
131	1	2180.584	122.157294	123.0744795
131.918	0.918	2178.085	123.0744795	123.9174218
132	0.082	2177.658	123.917422	123.9927323
133	1	2172.453	123.9927323	124.9133506
134	1	2167.248	124.9133506	125.8361799
135	1	2162.043	125.8361799	126.7612309
136	1	2156.383	126.7612309	127.6885142
137	1	2151.633	127.6885142	128.6180408
138	1	2146.428	128.6180408	129.5498214
139	1	2141.223	129.5498214	130.483867
140	1	2136.018	130.483867	131.4201887
140.706	0.706	2132.34	131.4201887	132.0823721
141	0.294	2126.838	132.0823721	132.3588388
142	1	2108.124	132.3588388	133.3075496
143	1	2089.41	133.3075496	134.2647576
144	1	2070.696	134.2647576	135.2306164
145	1	2051.982	135.2306164	136.2052838
146	1	2033.268	136.2052838	137.188922
147	1	2014.554	137.188922	138.1816975
148	1	1995.84	138.1816975	139.1837819
149	1	1977.126	139.1837819	140.1953512
150	1	1958.412	140.1953512	141.2165868
150.631	0.631	1946.601	141.2165868	141.8648963
151	0.369	1944.843	141.864896	142.2443611
152	1	1940.079	142.2443611	143.2752469
153	1	1935.315	143.2752469	144.3086704
154	1	1930.551	144.3086704	145.3446441
155	1	1925.787	145.3446441	146.3831806
156	1	1921	146.3831806	147.4242925
157	1	1916.259	147.4242925	148.4679928
158	1	1911.495	148.4679928	149.5142942
159	1	1906.731	149.5142942	150.5632099
160	1	1901.967	150.5632099	151.6147528
161	1	1897.203	151.6147528	152.6689363
162	1	1892.439	152.6689363	153.7257735
163	1	1887.675	153.7257735	154.7852779
164	1	1882.911	154.7852779	155.847463
165	1	1878.147	155.847463	156.9123424
166	1	1873.383	156.9123424	157.9799297
167	1	1868.619	157.9799297	159.0502389
168	1	1863.855	159.0502389	160.1232837

169	1	1859.091	160.1232837	161.1990783
170	1	1854.327	161.1990783	162.2776367
171	1	1849.563	162.2776367	163.3589732
172	1	1844.799	163.3589732	164.4431022
173	1	1840.035	164.4431022	165.530038
174	1	1835.271	165.530038	166.6197953
175	1	1830.507	166.6197953	167.7123888
176	1	1825.743	167.7123888	168.8078332
177	1	1820.979	168.8078332	169.9061435
178	1	1816.215	169.9061435	171.0073348
179	1	1811.451	171.0073348	172.111422
179.079	0.079	1811.86	172.111422	172.1986625
180	0.921	1807.853	172.1986625	173.2175512

APPENDIX B. UNIT DISTRIBUTION MAPS FOR PACKAGES -1 AND -2

The distribution of in Packages -1 and -2 were mapped from seismic data used in this study. The presence of unit is indicated by the color on the map. White space between the color are areas where the unit is not present or not imaged on the data.

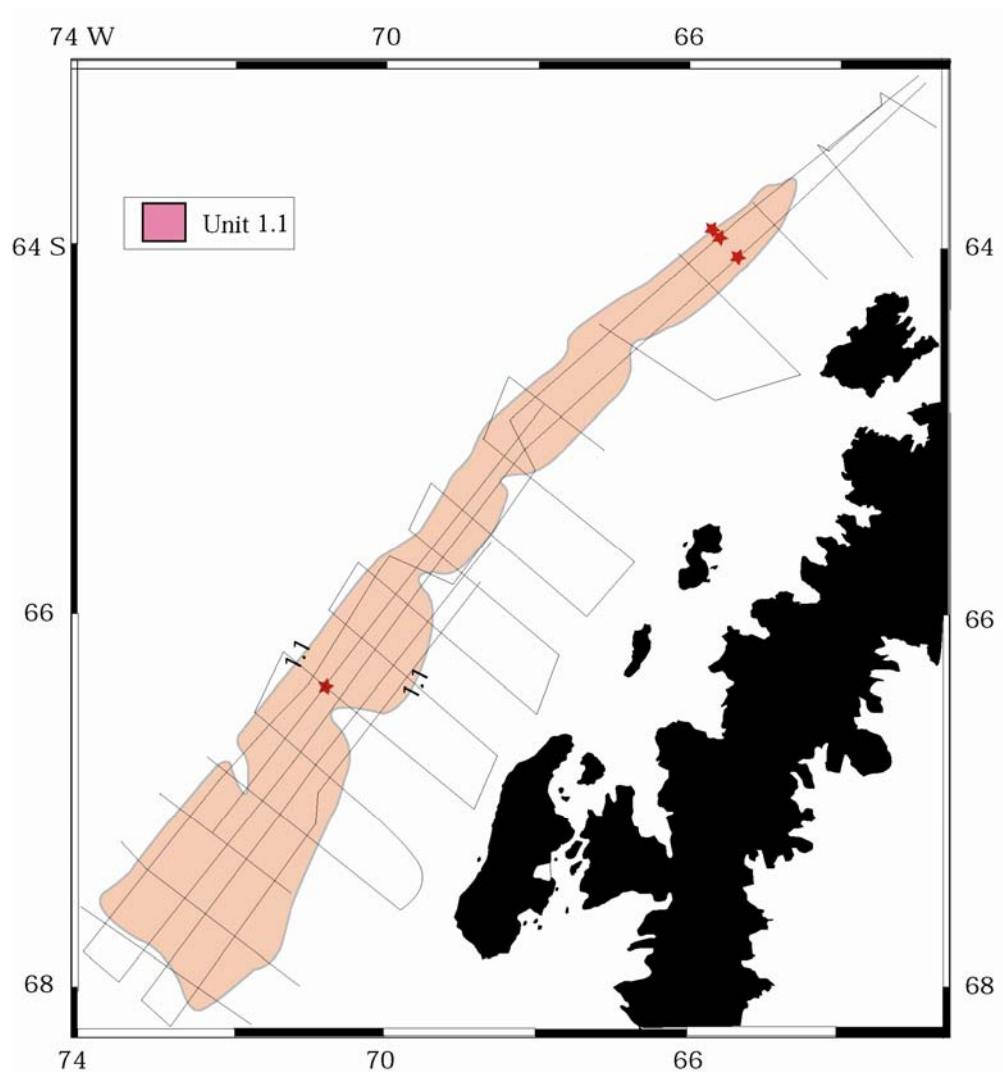


Figure 15b : Distribution map of unit 1.1 on the continental shelf. Many units overly each other, the absence of a unit is noted by the end of the black border around them.

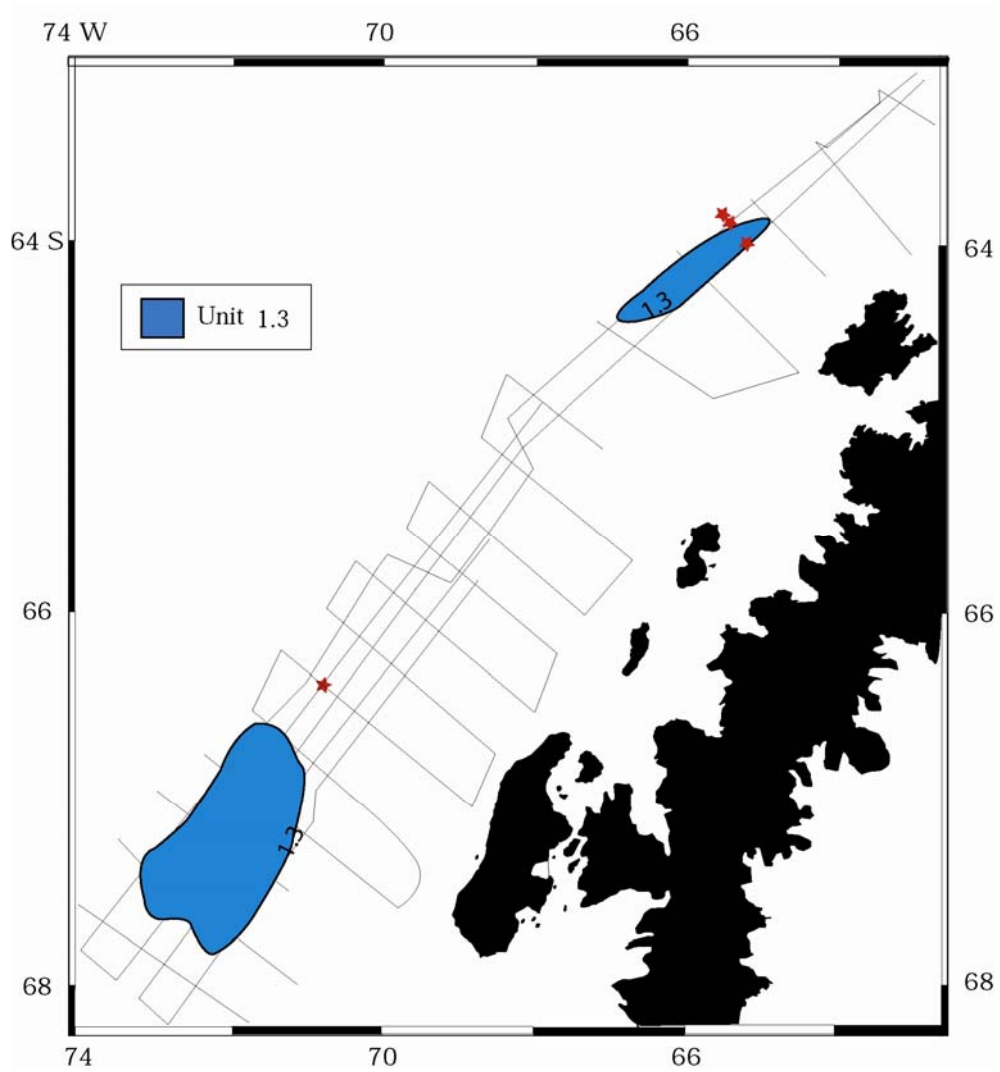


Figure 15c : Distribution map of unit 1.3 on the continental shelf. Many units overly each other, the absence of a unit is noted by the end of the black border around them.

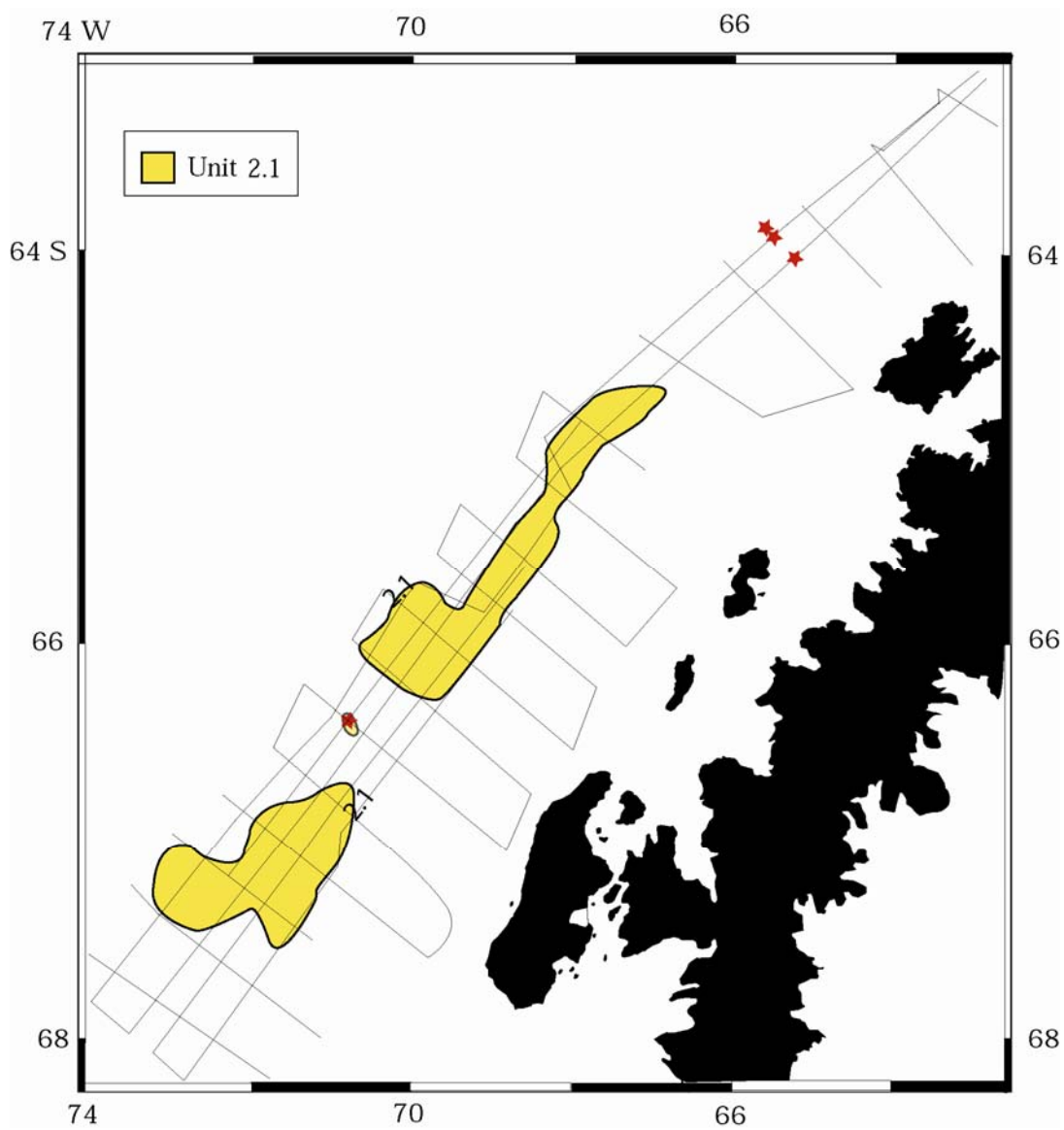


Figure 14b : Distribution map of unit 2.1 on the continental shelf. Absence of the unit is noted by the end of the black border around it.

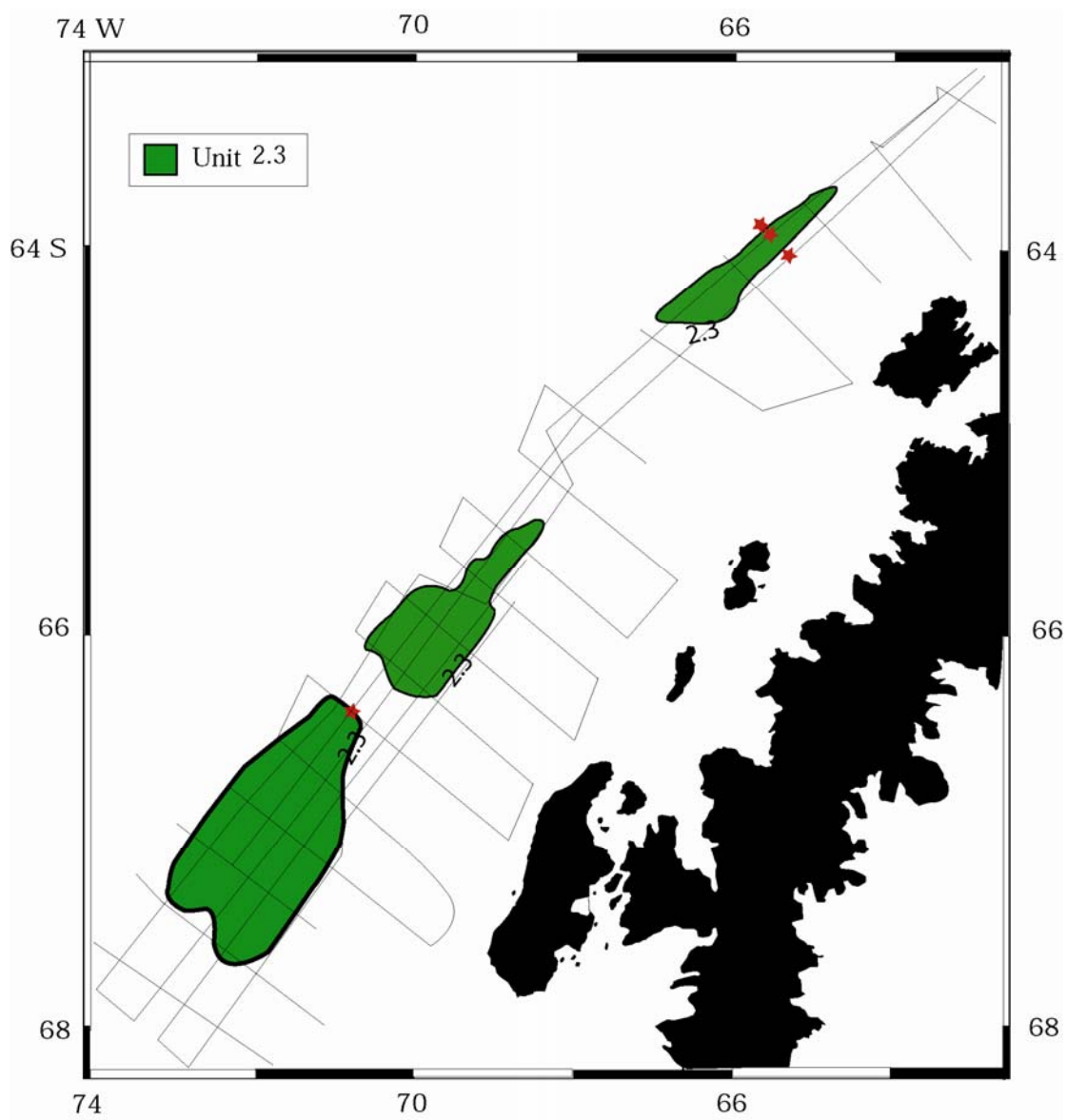


Figure 14c : Distribution map of unit 2.3 on the continental shelf. Absence of the unit is noted by the end of the black border around it.

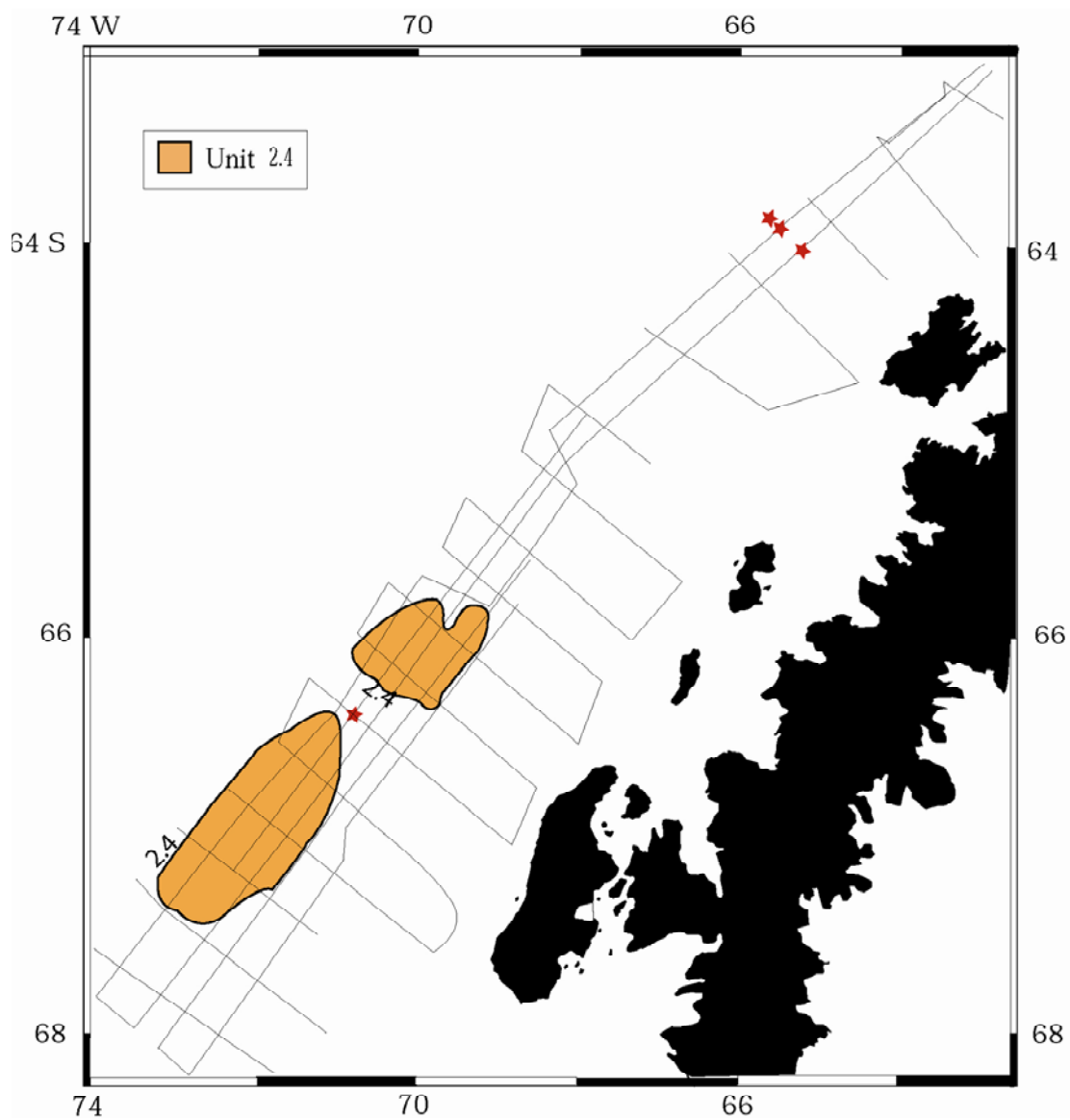


Figure 14d : Distribution map of unit 2.4 on the continental shelf. Absence of the unit is noted by the end of the black border around it.

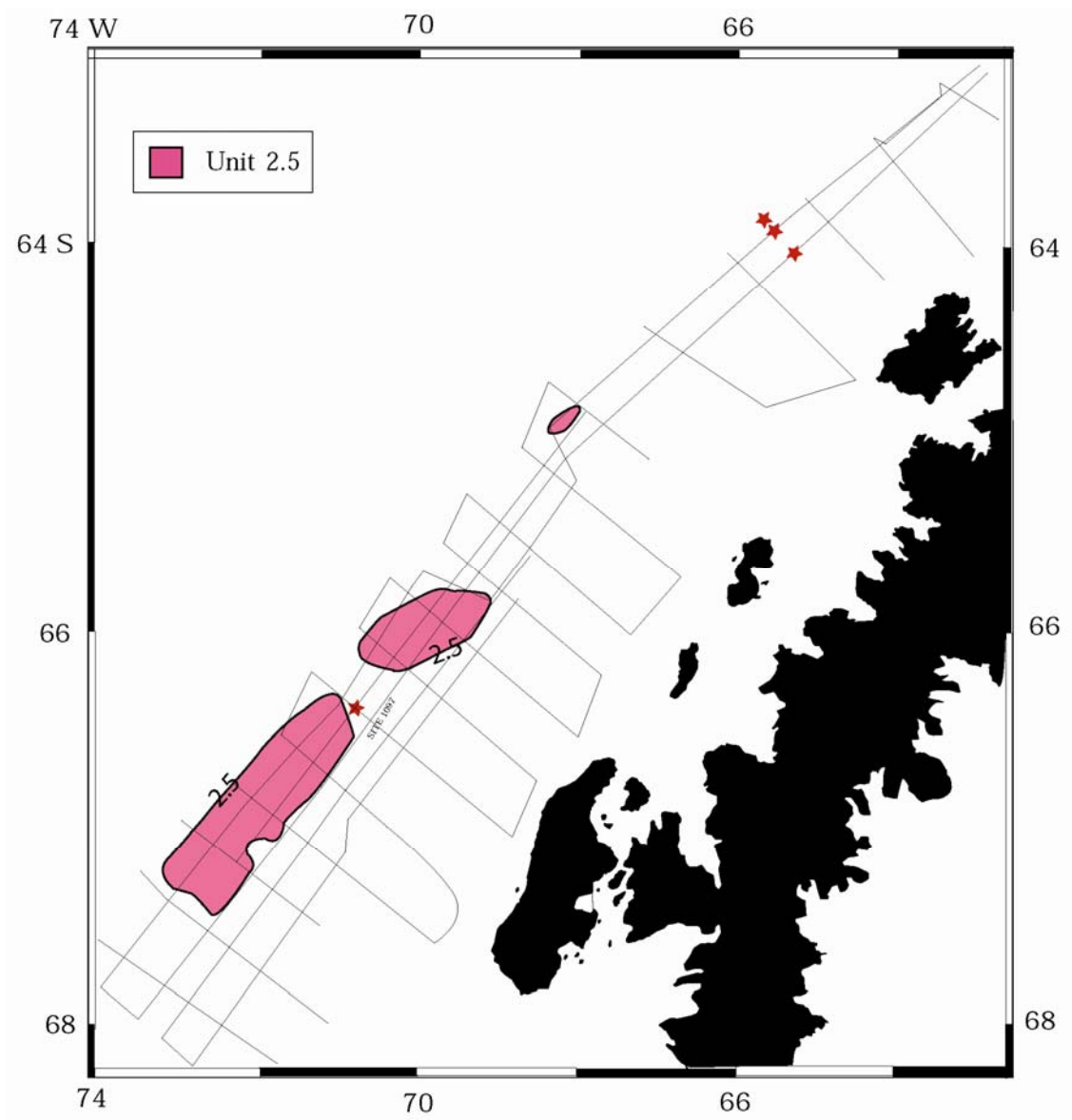


Figure 14e : Distribution map of unit 2.5 on the continental shelf. Absence of the unit is noted by the end of the black border around it.

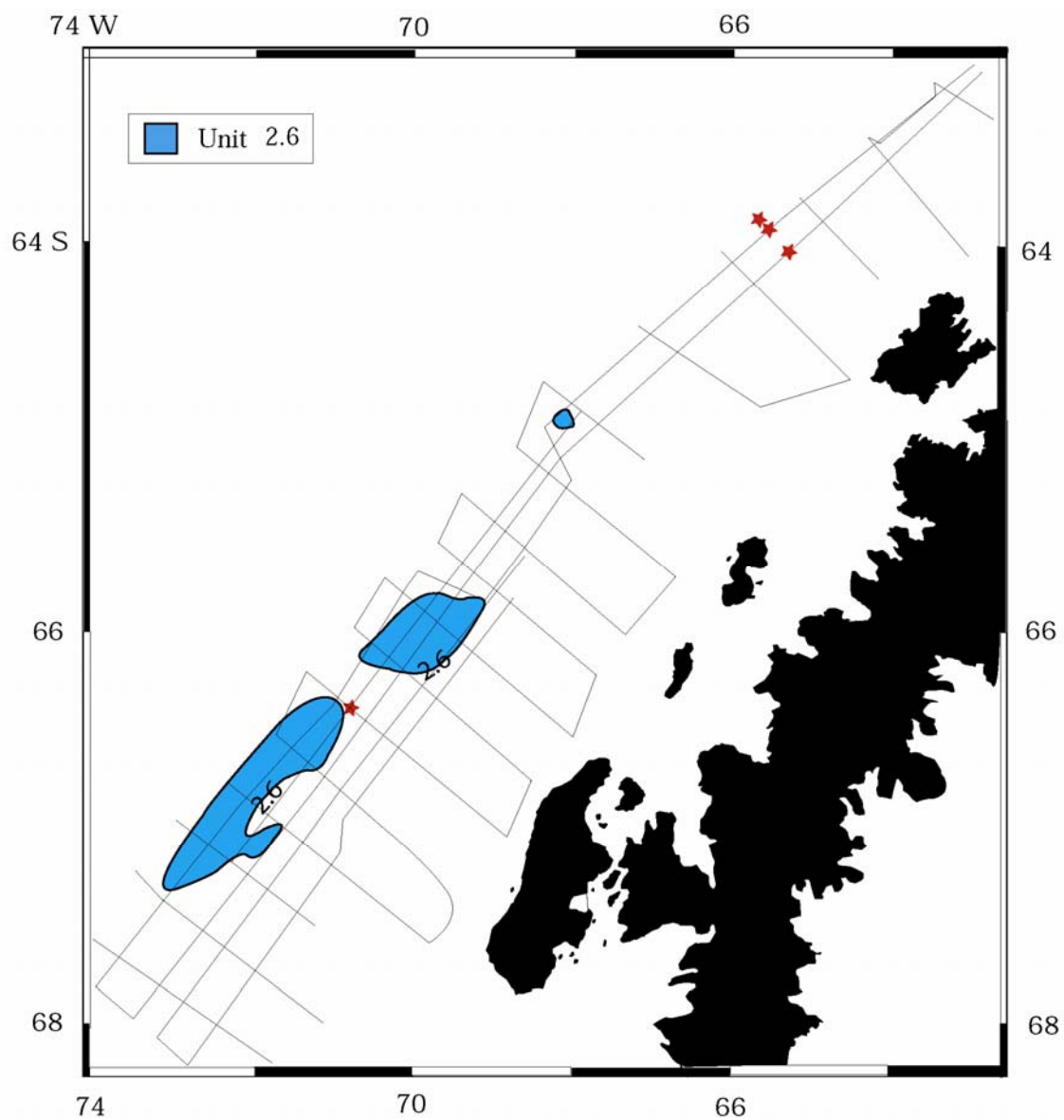


Figure 14f : Distribution map of unit 2.6 on the continental shelf. Absence of the unit is noted by the end of the black border around it.

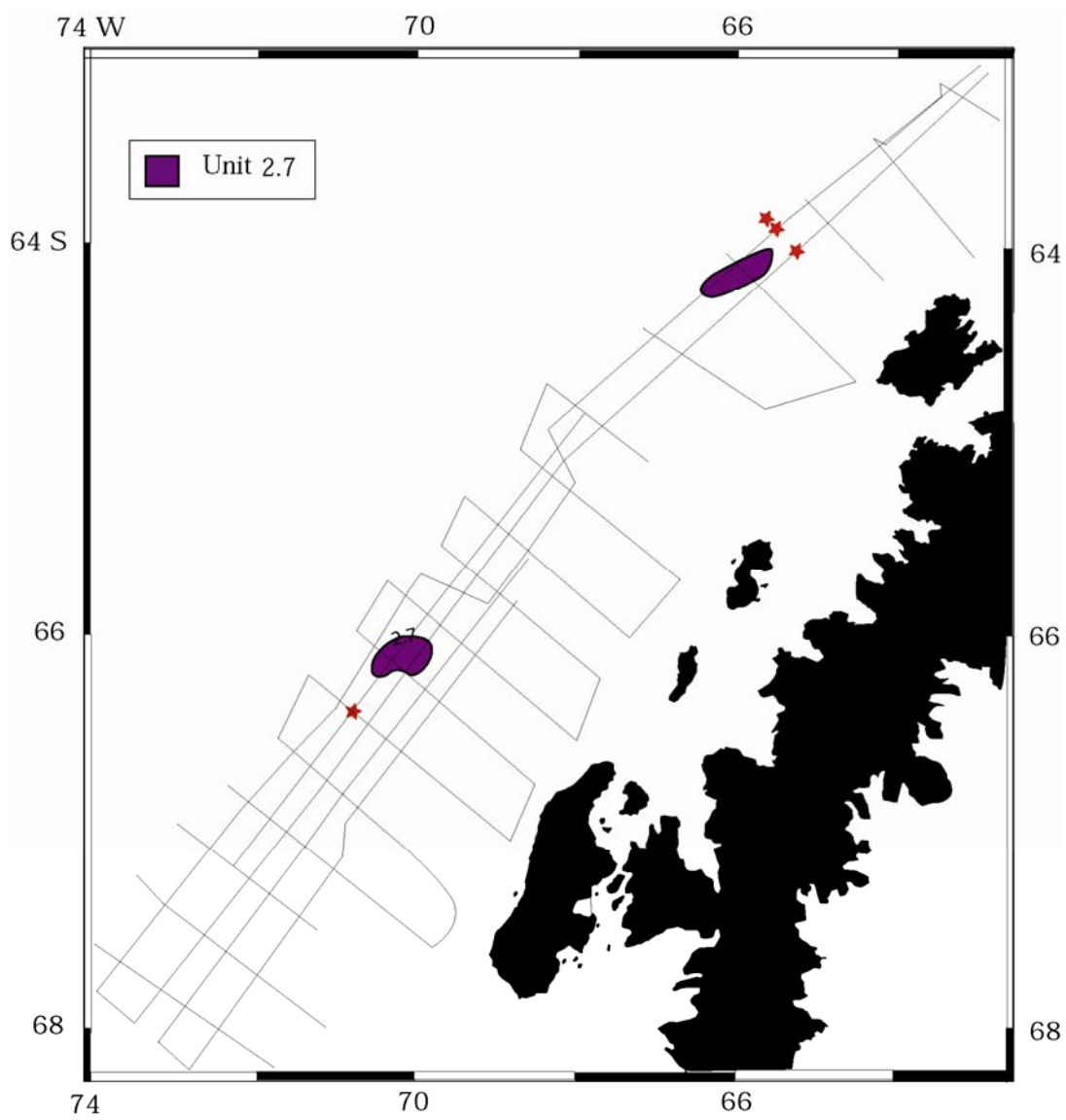


Figure 14g : Distribution map of unit 2.7 on the continental shelf. Absence of the unit is noted by the end of the black border around it.

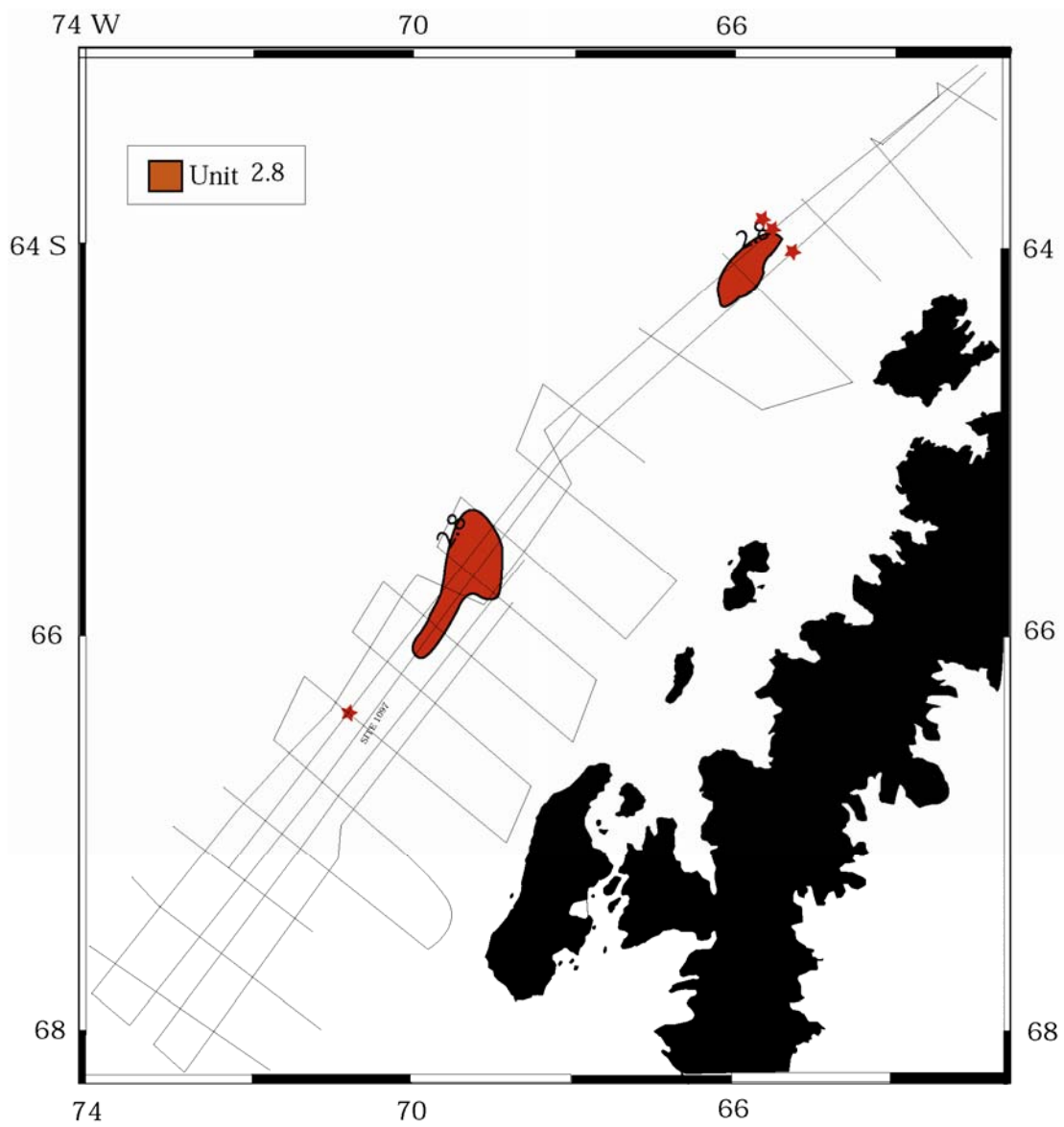


Figure 14h : Distribution map of unit 2.8 on the continental shelf. Absence of the unit is noted by the end of the black border around it.

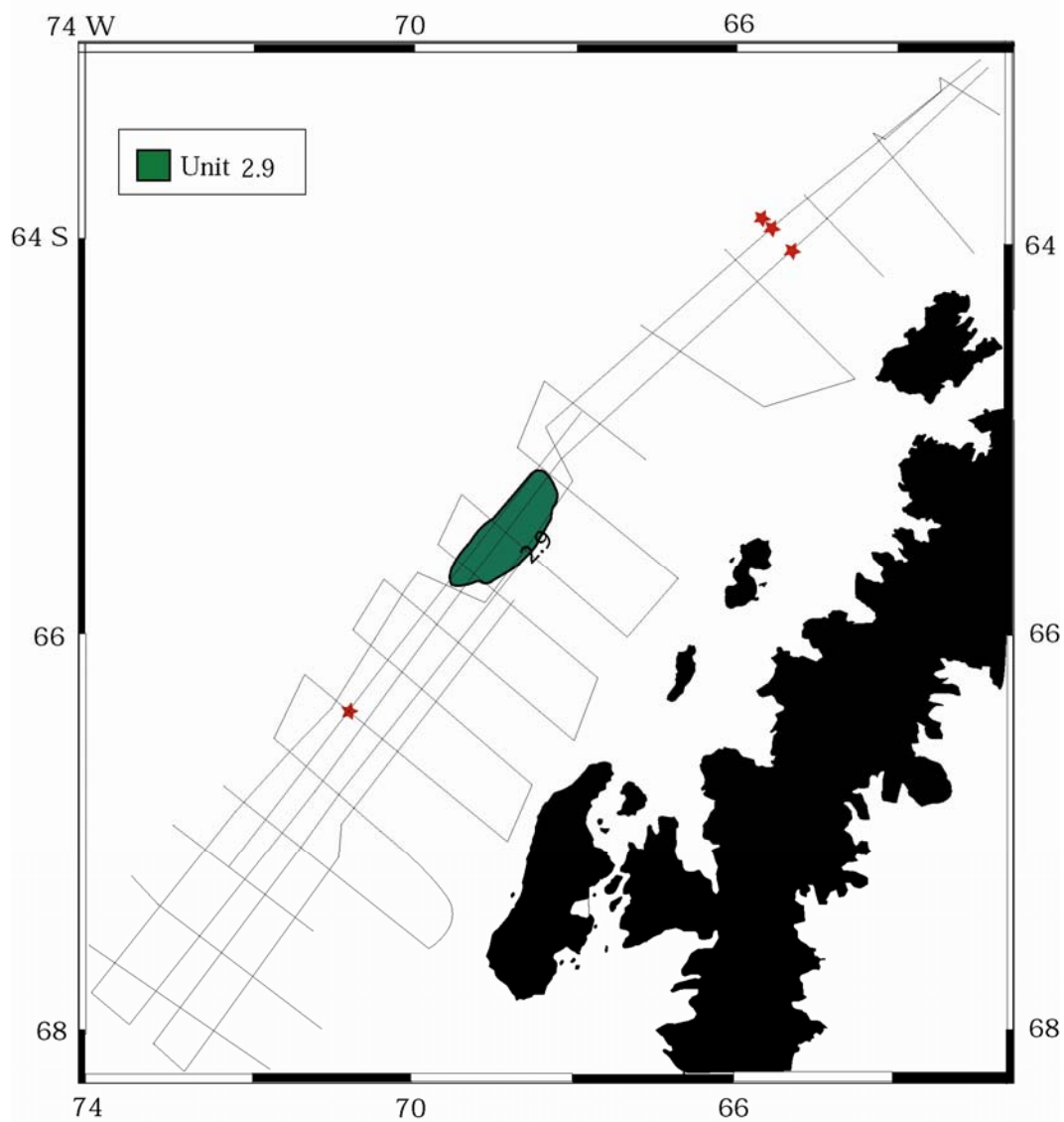


Figure 14i : Distribution map of unit 2.9 on the continental shelf. Absence of the unit is noted by the end of the black border around it.

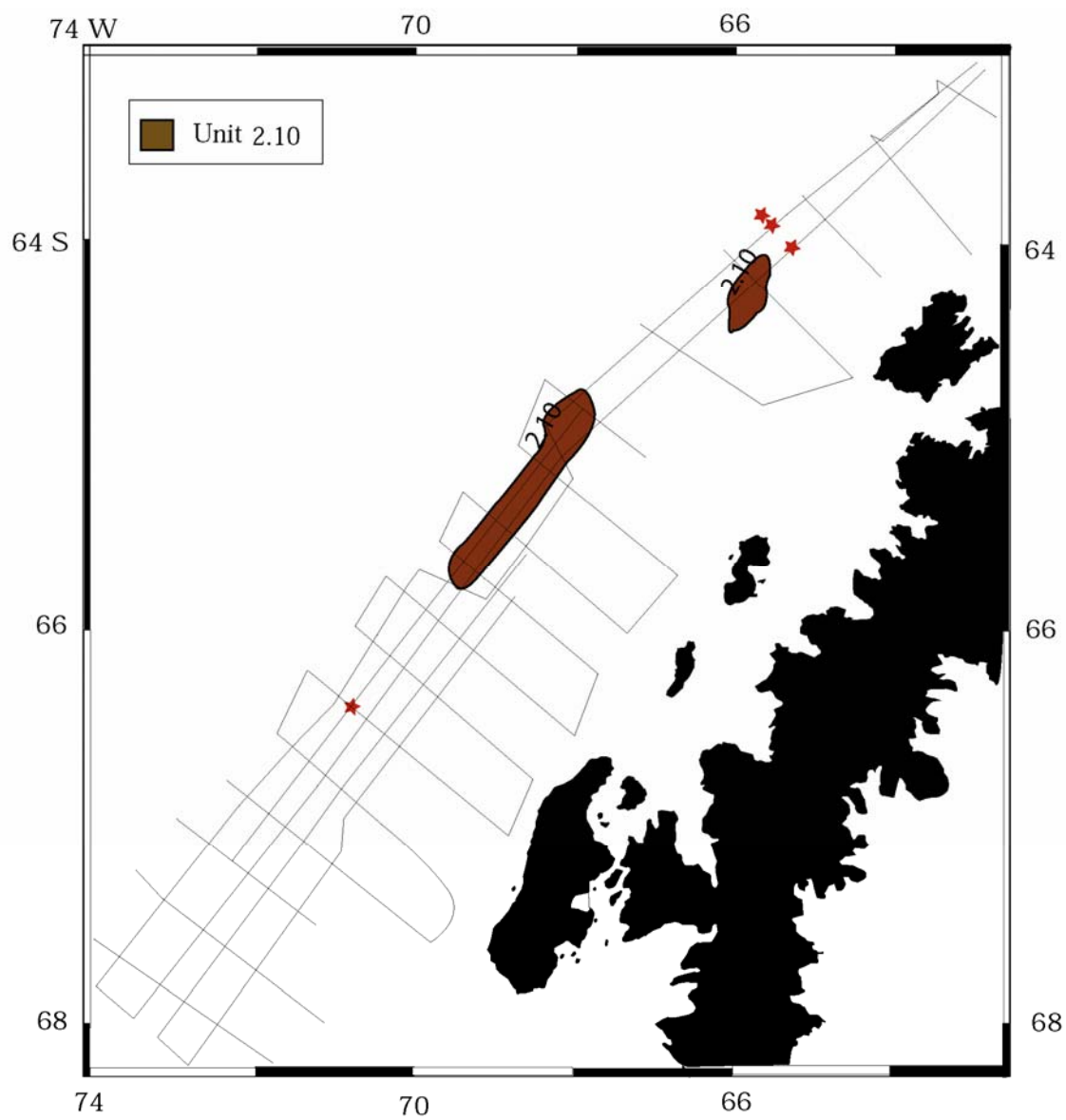


Figure 14j : Distribution map of unit 2.10 on the continental shelf. Absence of the unit is noted by the end of the black border around it.

VITA

Jason Henry Holloman was born in Houston, Texas, in 1980. A year later Jason moved with his family to Bloomington, Texas where he spent his entire childhood. A love of oil, livestock, sand and mud pushed Jason to science and eventually to geology. Putting the past to practical use in the present drives him through the everyday rigors he encounters.